AD_____

**AWARD NUMBER:** W81XWH-16-1-0334

**TITLE:** Transcriptional Modulation of Tumor-Associated Macrophages to Facilitate Prostate Cancer Immunotherapy

**PRINCIPAL INVESTIGATOR:** Alan Friedman, MD

**RECIPIENT:** Johns Hopkins University
Baltimore, MD 21218

**REPORT DATE:** September 2018

**TYPE OF REPORT:** Annual

**PREPARED FOR:** U.S. Army Medical Research and Materiel Command
Fort Detrick, Maryland 21702-5012

# REPORT DOCUMENTATION PAGE

*Form Approved*
*OMB No. 0704-0188*



| **1. REPORT DATE** *(DD-MM-YYYY)* | **2. REPORT TYPE** | **3. DATES COVERED** *(From - To)* |
|---|---|---|
| *September* 2018 | Annual Report | 1 SEP 2017 - 31 AUG 2018 |

**4. TITLE AND SUBTITLE**

Transcriptional Modulation of Tumor-Associated Macrophages to Facilitate Prostate Cancer Immunotherapy

**5a. CONTRACT NUMBER**

**5b. GRANT NUMBER**
W81XWH-16-1-0334

**5c. PROGRAM ELEMENT NUMBER**

**6. AUTHOR(S)**

Alan D. Friedman, M.D.
email:
afriedm2@jhmi.edu

**5d. PROJECT NUMBER**

**5e. TASK NUMBER**

**5f. WORK UNIT NUMBER**

**7. PERFORMING ORGANIZATION NAME(S) AND ADDRESS(ES)**

Johns Hopkins University
733 N. Broadway Suite 117
Baltimore, MD 21205

Johns Hopkins University
1650 Orleans Street, Room 253
Baltimore, MD 21287

**8. PERFORMING ORGANIZATION REPORT NUMBER**

**9. SPONSORING / MONITORING AGENCY NAME(S) AND ADDRESS(ES)**
U.S. Army Medical Research and Materiel Command
Fort Detrick, MD 21702-5014

**10. SPONSOR/MONITOR'S ACRONYM(S)**
DoD

**11. SPONSOR/MONITOR'S REPORT NUMBER(S)**

**12. DISTRIBUTION / AVAILABILITY STATEMENT**

Approved for public release; distribution unlimited

**13. SUPPLEMENTARY NOTES**

**14. ABSTRACT**

Prostate cancer (PCa) contains abundant tumor-associated macrophages (TAMs), with increased TAM M2 polarization correlating with disease stage, emergence of castration-resistance, and worse prognosis. We hypothesize that targeting TAM transcription factors that mediate their M2 polarization, reprogramming them into the pro-inflammatory M1 state, will provide a novel approach to PCa therapy, and we seek to assess whether adoptive transfer monocytes lacking a key TAM transcription factor shows therapeutic utility, alone or with checkpoint inhibition. During the current reporting year we found that a murine PCa line grows slower in mice lacking NF-kB p50 compared with wild-type controls and in KLF4(f/f);Lys-Cre mice vs KLF4(f/f) controls, with increased TAM M1 polarization, particularly in p50-/- hosts, and with increased number and activation of tumor T cells, predominantly CD4 T cells in p50-/- vs wild-type and CD8 T cells in KLF4(f/f);Lys-Cre vs KLF4(f/f) tumor recipients. We also demonstrated that expansion of marrow progenitors in SCF/FL/TPO for 6 days, culture in M-CSF for 1 day, and adoptive transfer allows PCa tumor localization in preference to normal organs. And we find that anti-PD-1 is active in our tumor model. Thus, we have identified two transcription factors whose down-regulation in PCa TAMs contributes to tumor control and have begun to optimize a novel immunotherapy including adoptive transfer of gene modified myeloid cells.

**15. SUBJECT TERMS**
Prostate cancer, immunotherapy, tumor-associated macrophages, NF-kB p50, KLF4

| **16. SECURITY CLASSIFICATION OF:** | | | **17. LIMITATION OF ABSTRACT** | **18. NUMBER OF PAGES** | **19a. NAME OF RESPONSIBLE PERSON** |
|---|---|---|---|---|---|
| **a. REPORT** | **b. ABSTRACT** | **c. THIS PAGE** | UU | | **19b. TELEPHONE NUMBER** *(include area code)* |
| U | U | U | | | |

**Transcriptional Modulation of Tumor-Associated Macrophages to Facilitate Prostate Cancer Immunotherapy**

## TABLE OF CONTENTS

**Page No.**

## 1. INTRODUCTION

Prostate cancer (PCa) contains abundant tumor-associated macrophages (TAMs), with their increased content and percentage of M2 polarization correlating with increased disease stage, emergence of castration-resistant disease, and worse prognosis. We hypothesize that targeting TAM transcription factors that mediate their M2 polarization, reprogramming them into the pro-inflammatory M1 state, would provide a novel approach to prostate cancer therapy. This project first seeks to determine whether syngeneic murine PCa cells, unselected or castration resistant, grow more slowly in mice lacking NF-κB p50 (p50), KLF4, or PU.1 in their myeloid cells, correlated with increased TAM M1 polarization and increased activation of tumor-infiltrating lymphocytes. We then seek to assess whether adoptive transfer or murine monocytes lacking p50, KLF4, or PU.1 slows PCa growth, alone or in synergy with CSF1R small molecule tyrosine kinase inhibitor (TKI) or antibody (Ab) targeting or with anti-PD-1 or anti-CTLA4 T cell checkpoint inhibitory antibodies.

## 2. KEYWORDS

Prostate cancer, immunotherapy, tumor-associated macrophages, NF-κB p50, KLF4

## 3. ACCOMPLISHMENTS

### Major goals of the project

Task 1: Assess prostate cancer growth in WT versus p50-/-, KLF4(f/f);Lys-Cre, and PU.1(kd/kd) B6 mice
- Subtask 1 - Obtain ACURO approval (mos 1-3), completed prior to 9/01/2016 start date
- Subtask 2 - Assess PCa growth in WT vs mutant recipients (mos 4-12), completed 6/01/17
- Subtask 3 - Assess castration-resistant growth in WT vs mutant recipients (mos 6-24), 75% complete
- Subtask 4 - Assess metastatic growth in WT vs mutant recipients (mos 6-24), 10% complete

Task 2: TAM polarization and T cell activation in WT vs p50-/-, KLF4(f/f);Lys-Cre, and PU.1(kd/kd) mice
- Subtask 1 - Obtain ACURO approval (mos 3-5), completed prior to 9/01/2016 start date
- Subtask 2 – Assess TAM polarization and T cell numbers and activation (mos 6-24), 90% complete.

Task 3: Assess the effect of adoptively transferred M2-defective M1 macrophages on prostate cancer
- Subtask 1 - Obtain ACURO approval (mos 2-5), completed prior to 9/01/2016 start date
- Subtask 2 - Determine effects of adoptively transferred monocytes (mos 6-24), completed 7/01/18
- Subtask 3 - Determine whether infused monocytes reach the tumor (mos 6-24), completed 7/01/18
- Subtask 4 - Determine how infused monocytes alter tumor TAMs and T cells (mos 6-24), 75% completed

Task 4: Assess synergy between CSF1R blockade and adoptive transfer of M2-defective M1 monocytes
- Subtask 1 - Obtain ACURO approval (mos 8-11), completed prior to 9/01/2016 start date
- Subtask 2 - Determine the effect of MCSFR TKI on prostate cancer growth (mos 12-36), 30% complete
- Subtask 3 - Determine synergy between MCSFR TKI and monocytes (mos 18-36), 0% complete
- Subtask 4 - Determine the effect of MCSFR TKI and monocytes on tumor TAMs/T cells (mos 18-36), 10%
- Subtask 5 - Determine synergy between MCSFR Ab and monocytes (mos 18-36), 10% complete
- Subtask 6 - Determine the effect of MCSFR Ab and monocytes on tumor TAMs/T cells (mos 18-36), 10%

Task 5: Assess synergy between checkpoint blockade and adoptive transfer of M2-defective M1 monocytes
- Subtask 1 - Obtain ACURO approval (mos 8-11), completed prior to 9/01/2016 start date
- Subtask 2 - Determine synergy between PD-1 Ab and monocytes on tumor growth (mos 12-36), 25%
- Subtask 3 - Determine synergy between CTLA4 Ab and monocytes on tumor growth (mos 12-36), 0%
- Subtask 4 - Determine synergy between PD-1/CTLA4 Ab and monocytes on tumor T cells (mos 12-36), 0%

**Accomplishments under these goals**

*Task 1/Subtask 2 - Assess prostate cancer growth in WT versus mutant mice*

Data showing significantly slowed Hi-Myc prostate cancer (PCa) growth in p50-/- versus WT and in KLF4(f/f);Lys-Cre vs KLF4(f/f) mice were provided in the Yr01 Progress Report. As noted in last year's report, it has been difficult to obtain male PU.1(kd/kd) mice in large numbers due to issues with breeding and viability. During Yr02, we were able to compare PCa tumor growth in a PU.1(kd/kd) male vs three WT males, finding no difference (**Fig. 1**).

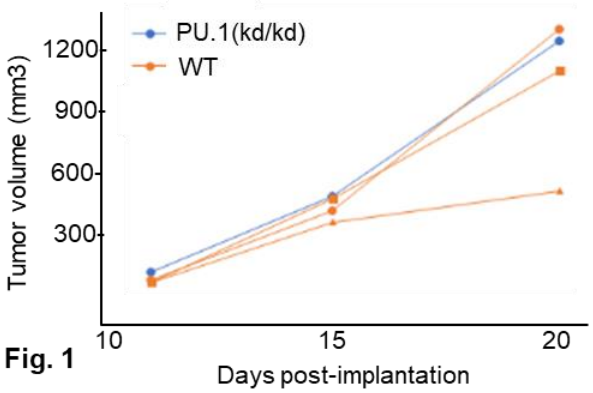


Fig. 1

*Task 1/Subtask 3 - Assess castration-resistant prostate cancer growth in WT versus mutant mice*

Data showing slowed castration-resistant prostate cancer (CRPC) in KLF4(f/f);Lys-Cre compared with KLF4(f/f) mice and development of a CRPC cell line that can be maintained by SQ passage was described in the Yr01 Progress Report. During Yr02 we compared CRPC growth in WT vs p50-/- tumor recipients, finding a trend toward slower growth in the absence of host NF-κB p50 (**Fig. 2**), with three outliers with very slow tumor growth preventing from our data thus far from reaching statistical significance.

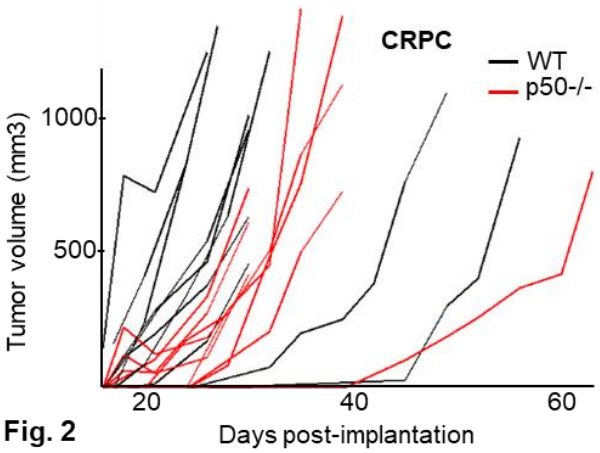


Fig. 2

*Task 2/Subtask 2 - Assess tumor TAM polarization and T cell numbers and activation in WT vs mutant hosts*

Data showing reduced M2 and increased M1 tumor-associated macrophage (TAM) polarization in p50-/- compared with WT hosts and in KLF4(f/f);Lys-Cre vs KLF4(f/f) PCa hosts was presented in the Yr01 Progress Report. In addition, data showing increased number and activation of tumor CD4 T cells in p50-/- hosts and increased number and activation of tumor CD8 T cells in KLF4(f/f);Lys-Cre hosts was provided. During Yr02, we demonstrated that CD8 T cell depletion via four CD8 Ab injections prior to tumor inoculation obviated the PCa growth difference in KLF4(f/f);Lys-Cre vs KLF4(f/f) hosts (**Fig. 3**).

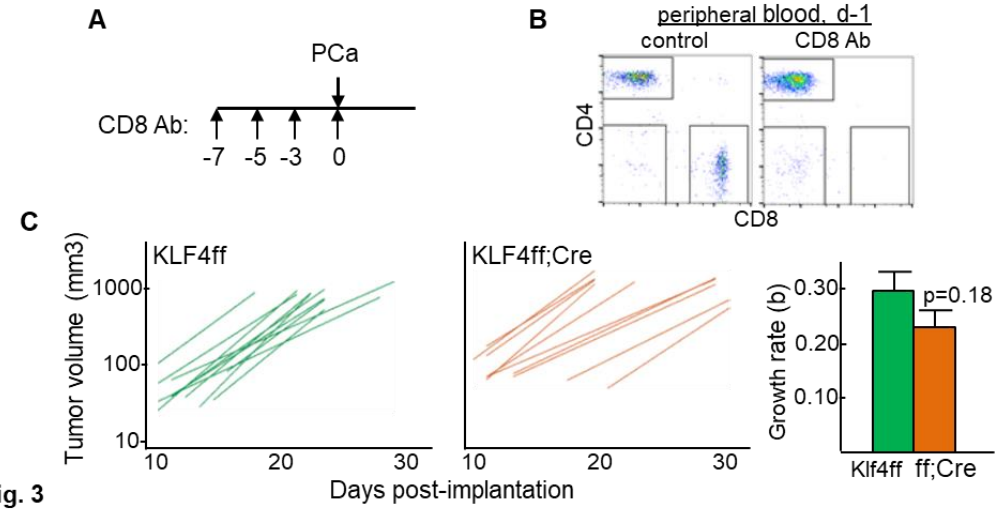


Fig. 3

Global gene expression analysis of $CD11b^+$ myeloid cells from PCa tumor growing in KLF4(f/f);Lys-Cre vs KLF4(f/f) hosts was also described in the Yr01 Progress Report. During Yr02, we completed Ingenuity Pathway Analysis of these data, finding that absence of KLF4 in PCa tumor myeloid cells leads to activation of pro-inflammatory Atherosclerosis Signaling as the top pathway activated (**Table 1**). These and earlier data regarding PCa growth in KLF4(f/f);Lys-Cre vs KLF4(f/f) mice were published during Yr02 (Barakat et al 2018).

**Table 1. Ingenuity Pathway Analysis of Klf4(f/f) vs Klf4(f/f);Lys-Cre PCa Myeloid Cells***

| **Pathway (-logB-H p-value)** | **RNAs higher in Klf4(f/f);Lys-Cre** | **RNAs higher in Klf4(f/f)** |
|---|---|---|
| Atherosclerosis Signaling (5.01) | Mmp3, CD36, Clu, Cma1, Col1a1, Col1a2, Col3a1, IL1rn, Rbp4, S100a8 | Lyz, Pdgfb, Tnf |
| LXR/RXR Activation (4.56) | Ahsg , CD36, Clu, IL1r2, IL1rn, Lbp, Rbp4, Vtn, S100a8 | Lyz, Nos2,Tnf |
| Granulocyte Adhesion and Diapedesis (3.98) | Ccl7, Cldn3, Cldn10, Fpr1, Hspb1 IL1r2, IL1rn, Mmp3, Pf4, Sell | Ccl24,Cxcl9,Tnf |
| Agranulocyte Adhesion and Diapedesis (3.79) | Acta2, Ccl7, Cldn3, Cldn10, IL1rn, Mmp3, Myl9, Pf4, Sell | Ccl24, Cxcl9, Fn1, Tnf |
| Hepatic Fibrosis/Hepatic Stellate Cell Activation (3.52) | Acta2, Ccr7, Col1a1, Col1a2, Col3a1, Igfbp5, IL1r2, Lbp, Myl9 | Fn1, Pdgfb, Tnf |
| Acute Phase Response Signaling (2.67) | Ahsg, C1r, Hp, IL1rn, Lbp, Rbp1, Rbp4, Saa3, Serping1 | Fn1, Tnf |
| Altered T Cell and B Cell Signaling in Rheumatoid Arthritis (RA) (2.67) | Spp1, IL1rn | HLA-DMA, HLA-DQA1, HLA-DRB5, Tlr12, Tnf, Tnfsf13b |
| Role of Macrophages, Fibroblasts and Endothelial Cells in RA (2.49) | Dkk3, , IL1r2, IL1rn, Mmp3, Sfrp2, Traf4 | Camk2d, Cebpe, Fn1, Nos2, Pdgfb, Prkcb, Tlr12, Tnf, Tnfsf13b |
| T Helper Cell Differentiation (2.49) | | Icosl, IL2ra, HLA-DMA, HLA-DQA1, HLA-DRB5, Tgfbr1, Tnf |
| Communication Between Innate and Adaptive Immune Cells (2.46) | Ccr7, IL1rn | HLA-DRB5, Ifnb1 Tlr12, Tnf, Tnfsf13b |

*Top 10 Ingenuity Pathways comparing mean RNA levels from $CD11b^+$ myeloid cells isolated from Hi-Myc PCa tumors in Klf4(f/f) vs Klf4(f/f)Lys-Cre hosts (n=2 per group).

*Task 3/Subtask 2 - Determine effects of adoptively transferred monocytes*
*Task 3/Subtask 3 - Determine whether infused monocytes reach prostate cancer tumors*

Data describing our ability to expand lineage-depleted ($Lin^-$) bone marrow cells in IMDM/FBS with TPO/SCF/FL for 6 days, followed by transfer to M-CSF or GM-CSF to generate immature myeloid cells (IMC) was described in the Yr01 Progress Report, together with data showing that IMC obtained using M-CSF but not GM-CSF localized to Hi-Myc PCa tumors. We made extensive progress during Yr02, characterizing IMC generated from p50-/- marrow (p50-IMC), demonstrating anti-PCa efficacy of p50-IMC compared to IMC generated from wild-type mice (WT-IMC), and characterizing effects of p50-IMC on PCa tumor myeloid and T cell activation, all contributing to an invention disclosure and to a provisional patent application submitted 5/30/18 for use of p50-IMC as a novel immunotherapy against PCa and other cancers.

We generate IMC as follows: Bone marrow flushed from the extremity bones is subjected to red blood cell lysis using ammonium chloride. Lineage-negative ($Lin^-$) cells are isolated using a magnetic column after staining with a cocktail of antibodies (CD3/B220/CD11b/Gr1/Ter119) that bind mature blood cells. These are then expanded for 6 days in IMDM media with fetal bovine serum (FBS) and the FL, TPO, and SCF cytokines. These cytokines maintain cell immaturity, leading to a blast-like morphology, as shown for cells expanded from the marrow of a p50-/- mouse (**Fig. 4A, left**). The cells are then transferred to IMDM/FBS, and M-CSF for 1 day, inducing an immature myeloid morphology in the majority of the cells (**Fig. 4A, right**). At this point ~87% of the cells express than pan-myeloid CD11b surface marker, with ~57% of $CD11b^+$ cells expressing the monocyte/macrophage marker CD115/MCSFR and ~22% instead expressing the dendritic cell (DC) markers Flt3/Flk2 and CD11c (**Fig. 4B**). 6% of the cells express the Ly6G granulocyte marker, and none express the CD3 T cell or CD19 B cell markers (not shown). Cells obtained using the same protocol using WT marrow have similar morphologic and FACS characteristics.

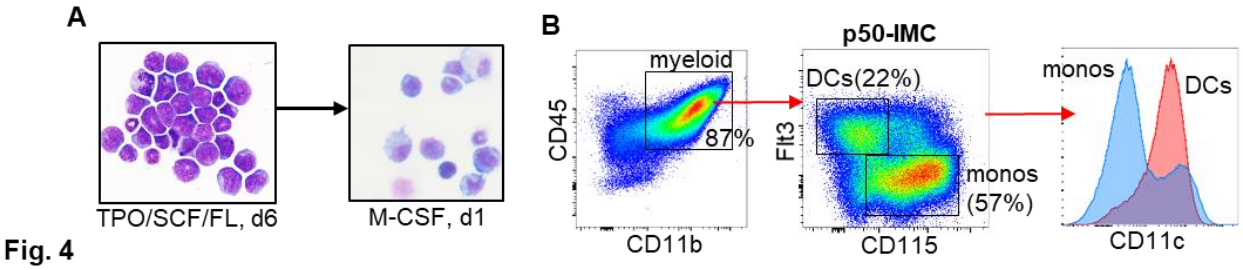

Fig. 4

We generated WT-IMC from CMV-Luc mice harboring a luciferase transgene (Jackson Labs). When a single dose of WT-IMC was infused into PCa tumor-bearing mice, 5 days after a dose of 5-fluorouracil (5FU, 150 mg/kg i.p.), a subset of cells reach the tumor, with cells also localizing to lung, spleen, and bone marrow (**Fig. 5A**). 5FU is given to reduce marrow production of blood monocytes that can compete with IMC for tumor localization, to reduce tumor myeloid cell numbers, and to release tumor neoantigens that might favor an immune response.

To quantify tumor localization and to evaluate the *in vivo* fate of p50-IMC, we have taken advantage of the CD45.1/CD45.2 congenic allele pair. WT CD45.1 mice inoculated with PCa cells received 5FU followed by a single dose of $CD45.2^+$ p50-IMC by tail vein injection. ~2% of tumor, and 13% of BM, 24% of spleen, and 1.4% of inguinal node $CD11b^+$ myeloid cells derived from $CD45.2^+$ p50-IMC (**Fig. 5B**). The majority of PCa tumor $CD45.2^+CD11b^+$ cells express F4/80, CD11c, and MHCII, indicative of activated macrophages and/or DCs, whereas few tumor $CD45.2^+CD11b^+$ cells express the granulocytic Ly6G marker (**Fig. 5C, top**), and a similar pattern was seen within the draining inguinal nodes (not shown). In contrast, p50-IMC-derived marrow cells express variable F4/80 and little CD11c or the MHCII activation marker, with a prominent $Ly6G^+$ subset, indicative of donor-derived macrophages and granulocytes (**Fig. 5C, bottom**), and a similar pattern was evident in spleen (not shown). Thus, p50-IMC form activated tumor and lymph node myeloid cells, with marrow and spleen potentially providing an ongoing reservoir.

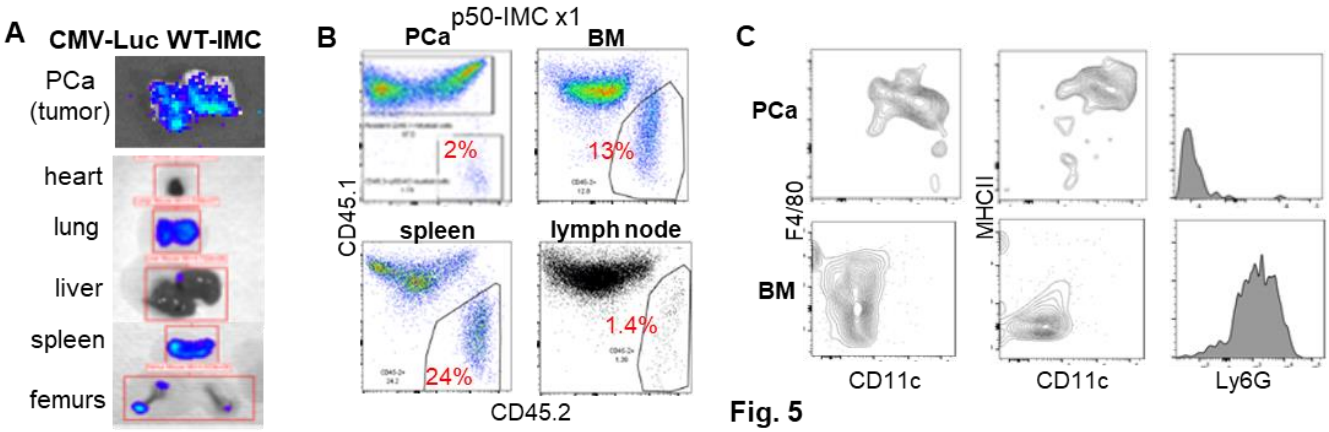

Fig. 5

To determine the effect of p50-IMC on T cell activation, in a separate experiment CD45.1$^+$ mice inoculated with Hi-Myc PCa received 5FU on d13 followed by 1E7 CD45.2$^+$ WT-IMC or p50-IMC on days 18, 21, and 25, followed by isolation of tumor and inguinal nodes six days later. Total tumor CD8 T cells were increased 5-fold by p50-IMC (**Fig. 6A**), with ~2-fold increase in IFNγ$^+$, activated CD8 T cells evident after 4 hr stimulation with PMA/ionomycin (**Fig. 6B**). Similarly, 7.7% of lymph node CD8 T cells expressed IFNγ after WT-IMC compared with 14.7% after p50-IMC, in response to PMA/ionomycin (p=0.004), and 1.8% of lymph node CD4 T cells were IFNγ$^+$ after WT-IMC compared with 5.3% after p50-IMC (p=0.007, not shown). In addition, the percent of tumor CD8 T cells expressing PD-1 increased almost 2-fold after p50-IMC (**Fig. 6C**), supporting the potential utility of combining p50-IMC with anti-PD-1 antibody.

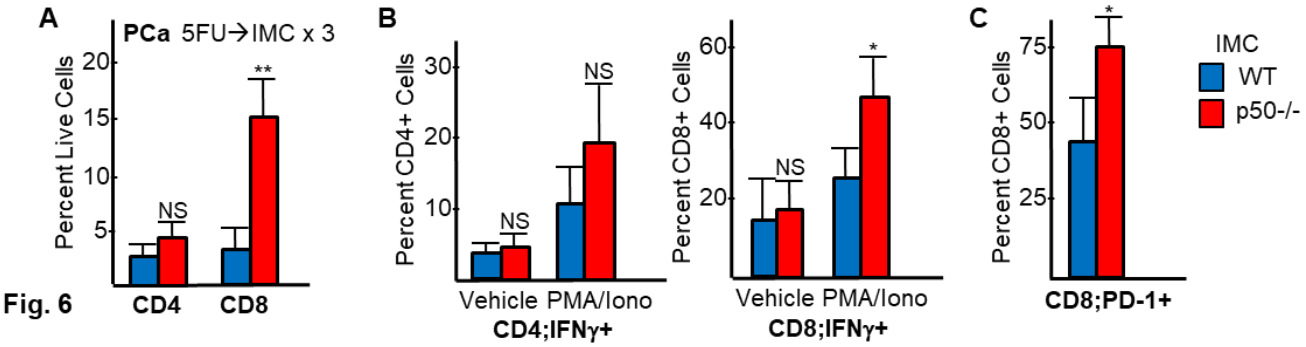


Fig. 6

Finally, we have evaluated the anti-tumor efficacy of 5FU alone, 5FU followed by 3 doses of p50-IMC, versus 5FU followed 3 doses WT-IMC. IMC were given via tail vein injection, 1E7 cells/dose, 2-4 days apart, starting 5d after a single dose of 5FU. Strikingly, Mice inoculated with Hi-Myc PCa showed significantly slower tumor growth after receiving 5FU on day 13 followed by p50-IMC on days 18, 21, and 25, compared to mice receiving 5FU and then WT-IMC or mice receiving 5FU alone (**Fig. 7A**). While 5FU alone slows PCa growth (and p50-IMC adds efficacy to this), provision of p50-IMC without 5FU did not lead to slowed tumor growth (**Fig. 7B**).

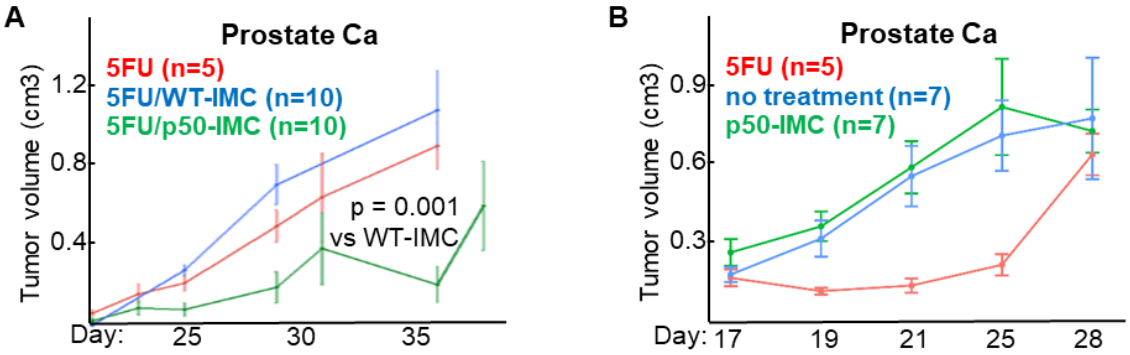


Fig. 7

*Task4/Subtask 2 - Determine the effect of MCSFR TKI on prostate cancer growth*
*Task4/Subtask 4 - Determine the effect of MCSFR TKI and monocytes on tumor TAMs/T cells*
*Task 4/Subtask 6 - Determine the effect of MCSFR Ab and monocytes on tumor TAMs/T* cells

The Yr01 Progress Report presented data indicating that MCSFR Ab could be detected in serum 2 days but not 6 days after three i.p. injections, based on the ability serum to stain exogenous MCSFR expressed on the surface of Ba/F3 cells. We concluded that IMC infusions will need to be delayed 5-6 days post-MCSFR Ab. During Yr02, we evaluated the effect of MCSFR Ab and of PLX3397, an MCSFR tyrosine kinase inhibitor (TKI), on PCa tumor myeloid cell numbers and tumor growth. Mice inoculated with Hi-Myc PCa were given MCSFR Ab (0.5 mg ip) on days 14, 16, and 18 or PLX3397 (50 mg/kg/day) by oral gavage on days 14-18, followed by analysis of tumor myeloid cells on day 21 (**Fig. 8**). MCSFR Ab reduced total and F4/80$^+$ tumor myeloid cells ~2-fold, whereas PLX3397 had little effect. MCSFR Ab did not affect tumor growth, with a trend towards smaller tumors with TKI (not shown).

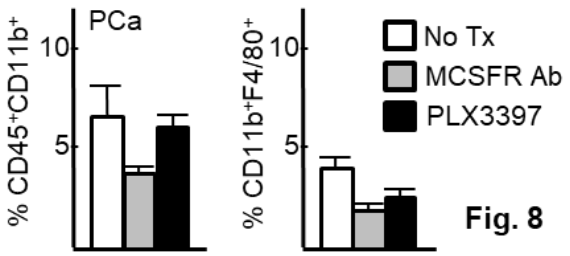


Fig. 8

*Task 5/Subtask 2 - Determine synergy between PD-1 Ab and monocytes on tumor growth*

The Yr01 Progress Report presented data showing that absence of host myeloid KLF4 or three dose of anti-PD-1 Ab (250 μg/dose) markedly slows PCa tumor growth, with the combination leading to a further mild reduction in tumor volume. In an effort to better demonstrate synergy, during Yr02 we repeated this experiment using one 250 μg dose of anti-PD-1 (**Fig. 9A**). There was a trend toward slowed tumor growth when anti-PD-1 Ab was combined with absence of myeloid KLF4. During Yr02 we also evaluated synergy between 5FU/p50-IMC and three doses of anti-PD-1 Ab (**Fig. 9B**), finding no evidence for cooperation under this protocol.

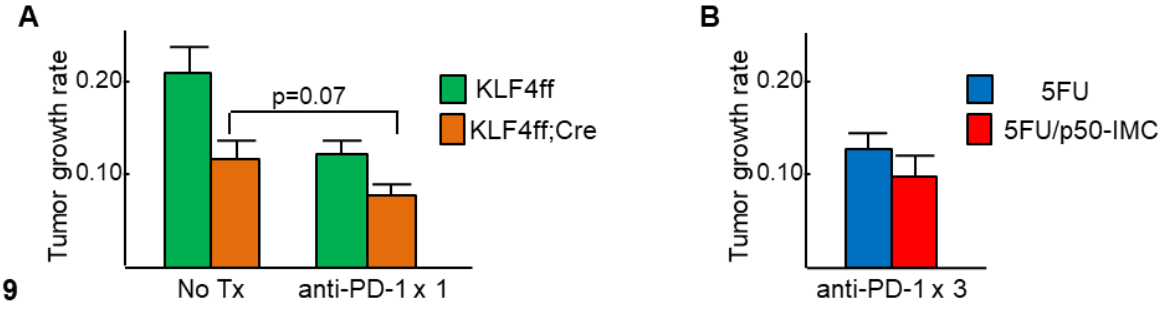


**Fig. 9**

**Opportunities for training and professional development**

During the past year, this proposal facilitated laboratory-based training and professional development in the fields of prostate cancer research and immunotherapy for two post-doctoral fellows, David Barakat, Ph.D. and Rahul Suresh, Ph.D. In addition to conducting the above experiments, Drs. Barakat and Suresh attended and presented at weekly laboratory meeting held by Drs. Friedman and Pienta, and attended numerous scientific seminars at the Johns Hopkins Comprehensive Cancer Center, including Oncology Grand Rounds, Translational Research Conference, and Journal Club. Dr. Suresh presented his findings regarding the efficacy of p50-IMC against PCa as a poster presentation at the Johns Hopkins Prostate Cancer Research Day symposium (12/07/2017) and at the Johns Hopkins Cancer Center Fellow Research Day symposium (6/14/2018).

**Dissemination of research results**

Nothing to Report.

**Plans during the next reporting period**

*Task 1* Given the promising findings presented in Fig. 3, we will obtain additional CRPC tumor growth data in WT vs p50-/- mice, as well as in KLF4(f/f) vs KLF4(f/f);Lys-Cre mice. We will also will inoculate these mice with Hi-Myc PCa cells, and once tumors reach 1.2-1.4 cm will remove the tumors and then assess lung metastases 6 wks later.

*Task 2* We will assess CRPC tumor myeloid and T cell numbers and activation in WT vs p50-/- and KLF4(f/f) versus KLF4(f/f);Lys-Cre Hi-Myc PCa tumor recipients, using FC and qRT-PCR analysis of isolated tumor $CD11b^+$ myeloid cells.

*Task 3* We will conduct additional experiments to characterize the effects of 5FU followed by p50-IMC infusions on PCa tumor myeloid and T cell activation, including repeating the experiments presented in Fig. 5C and Fig. 6 and isolation of tumor $CD11b^+$ myeloid cells after 5FU, 5FU/p50-IMC, or 5FU/WT-IMC followed by FC and qRT-PCR analysis for markers of M1 vs M2 tumor myeloid cell polarization.

*Task 4* WT mice inoculated with Hi-Myc PCa 14d earlier will be treated with PLX3397 by oral gavage (50 mg/kg/day x 4 days), alone or with subsequent 5FU and then three dose of p50-IMC, followed by assessment of tumor growth and tumor TAM and T cell phenotypes. We will also expose mice inoculated with Hi-Myc PCa to MCSFR Ab, alone or preceding 5FU/p50-IMC by 6 days, followed by assessment of tumor growth and tumor TAM and T cell phenotypes. An additional control group will receive 5FU/p50-IMC alone.

*Task 5* To extend promising findings in Fig. 9, we will inoculate KLF4(f/f) vs KLF4(f/f);Lys-Cre mice with Hi-Myc PCa, followed by one dose of anti-PD-1 antibody on day 14, followed by monitoring of tumor growth. We will also conduct a related experiment using one dose of anti-PD-1 with WT vs p50-/- tumor recipients. We will also conduct this experiment using anti-CTLA4 antibody alone or combined with anti-PD-1. In addition, we will combine one dose of anti-PD-1 Ab, anti-CTLA4 Ab, or both with 5FU/p50-IMC.

## 4. IMPACT

**Impact on the development of the principal discipline(s) of the project**

Prostate cancers include normal white blood cells called macrophages that contribute to tumor growth. These tumor-associated macrophages (TAMs) suppress the immune system's ability to fight prostate cancer. This proposal seeks to alter prostate cancer TAMs so that instead of helping the cancer grow they now help the immune system fight the cancer. Like all cells, TAMs contain genes within their DNA that govern their function. Our results indicate that removal of the KLF4 gene or the p50 gene from prostate cancer TAMs slows prostate cancer growth. In addition, we find that intravenous infusion of white blood cells lacking p50 into normal mice slows the growth of prostate cancer. These findings have implications for the treatment of prostate cancer, as we can now pursue a therapy in which we target KLF4 or p50 in TAMs, either within the tumor or in myeloid cells prior to their infusion.

**Impact on other disciplines**

In addition to prostate cancer, many other cancer contain TAMs that contribute to tumor growth, including brain, pancreatic, and breast cancers. Our findings are therefore also relevant to these and other cancers as targeting TAM KLF4 or p50 may also be effective for these cancers, alone or in combination with other therapies.

**Impact on technology transfer**

Our invention of p50-IMC and demonstration of efficacy against PCa when given after 5FU, has the potential to lead to transfer to industry and ultimately to clinical practice in patients with prostate cancer and other malignancies.

**Impact on society beyond science and technology**

Nothing to Report.

## 5. CHANGES/PROBLEMS

**Changes in approach**

Nothing to Report.

**Actual or anticipated problems or delays and actions or plans to resolve them**

We have yet to establish the Hi-Myc PCa metastasis model, wherein removal of sq tumors once large is intended to prolong survival and enable development of lung nodules at ~6 wks. We will continue to optimize this model by euthanizing mice at different time points after primary tumor removal (e.g. 6 wks, 9, wks, 12 wks, 15 wks, 18 wks) to find the time point at which lung nodules develop. We will then apply this assay to WT vs p50-/- and KFL4(f/f/) vs KLF4(f/f);Lys-Cre mice.

**Changes that had a significant impact on expenditures**

Nothing to Report.

**Significant changes in use or care of human subjects, vertebrate animals, biohazards, and/or select agents**

Nothing to Report.

## 6. PRODUCTS

### Journal publications

The following peer-reviewed research manuscript was published during Yr02:

*Authors* Barakat DJ, Suresh R, Barberi T, Pienta K, Simons BW, Friedman AD.
*Title* Absence of myeloid Klf4 reduces prostate cancer growth with pro-atherosclerotic activation of tumor myeloid cells and infiltration of CD8 T cells.
*Journal* PLoS One
*Volume:year* 13:2018
*Page numbers* e0191188 (16 pages)
*Status of publication* published
*Acknowledgment of federal support* Yes

### Books or other non-periodical, one time publications

Nothing to Report.

### Other publications, conference papers, and presentations

The following poster was presented at the 12th Annual Johns Hopkins Prostate Research Day on Dec. 7, 2017:

Suresh R, Barakat DJ, Gilmore GL, Simons B, Pienta KJ, Friedman AD. "Adoptive Transfer of Reprogrammed Myeloid Cells As a Component of Prostate Tumor Immunotherapy."

The following poster was presented at the Johns Hopkins University School of Medicine 2018 Sidney Kimmel Comprehensive Cancer Center Fellow Research Day on June 14, 2018:

Suresh R, Barakat DJ, Gilmore GL, Simons B, Pienta KJ, Friedman AD. "Adoptive Transfer of NF-kB Deficient Myeloid Cells As a Component of Prostate Cancer Immunotherapy."

### Websites or other internet sites

Nothing to Report.

### Technologies or techniques

Nothing to Report.

### Inventions and Patent Applications

An Invention Disclosure, "Adoptive Cell Transfer of NF-κB p50 Deficient Immature Myeloid Cells (ACT of p50-IMC)" was made to iEDISON by the Johns Hopkins Technology Ventures (JHTV) office ~4 weeks after initial disclosure to JHTV. The iEDISON EIR# is 4134401-18-0009.

A provisional patent application, #62677815, was made on May, 30, 2018 to the United States Patent and Trademark Office entitled "NF-κB p50 Deficient Immature Myeloid Cells and Their Use in Treatment of Cancer."

### Other products

*Data* We find that prostate cancer grows significantly slower in mice lacking NF-κB p50 or macrophage KLF4, or in mice with prostate cancer that are given 5FU followed by p50-IMC, associated with increased tumor macrophage and T cell activation. These findings provide a meaningful contribution towards understanding gene regulatory mechanisms that allow TAMs to contribute to prostate cancer growth and towards developing of novel therapy approaches designed to modify tumor TAMs.

*Research materials* We have developed a C57BL/6 murine cell line model of castration-resistant prostate cancer (CRPC) from castration-sensitive B6 Hi-Myc PCa.

## 7. PARTICIPANTS AND OTHER COLLABORATING ORGANIZATIONS

**Individuals who worked on the project (effort round up to nearest whole month)**

Name: Alan D. Friedman
Project Role: Principal Investigator
Person months worked: 1
Contribution to Project: no change
Funding Support: this award

Name: Kenneth J. Pienta
Project Role: Co-investigator
Person months worked: 1
Contribution to Project: no change
Funding Support: this award

Name: David Barakat
Project Role: Post-doctoral Fellow
Person months worked: 8
Contribution to Project: no change
Funding Support: this award

Name: Rahul Suresh
Project Role: Post-doctoral Fellow
Person months worked: 4
Contribution to Project: no change
Funding Support: this award

**Change in the active other support of the PI and senior/key personnel**

Name: Alan D. Friedman
Changes: closed
80039689, Allegheny Health Network-Johns Hopkins Cancer Research Fund

Name: Kenneth J. Pienta
Changes: closed
U54CA163214, NIH
1UM1HG006508, NIH
90055958, Prostate Cancer Foundation
90069213, CelSee
90065394, Harvard/DFCI sub-award

new
R02CA211695, NIH (Hurley, Paua), 12/01/17-11/30/22, 0.36 Cal

Dr. Pienta's 0.12 Cal annual effort on this DoD award (contract #W81XWH-16-1-0334) will not change as a result of his new Other Support.

**Other organizations involved as partners**

Nothing to Report.

## 8. SPECIAL REPORTING REQUIREMENTS

Not applicable.

## 9. APPENDICES

1. Barakat et al., PLoS One, 2018; 13:e0191188 (journal publication)
2. Suresh et al. (abstract of presentation at Johns Hopkins Cancer Center Fellow Research Day, June, 2018).
3. Friedman AD. NF-κB p50 Deficient Immature Myeloid Cells and Their Use in Treatment of Cancer. (provisional patent application)

PLOS ONE

RESEARCH ARTICLE

# Absence of myeloid Klf4 reduces prostate cancer growth with pro-atherosclerotic activation of tumor myeloid cells and infiltration of CD8 T cells

**David J. Barakat[1], Rahul Suresh[1], Theresa Barberi[1], Kenneth J. Pienta[1,2], Brian W. Simons[2], Alan D. Friedman[1]***

**1** Department of Oncology, Johns Hopkins University School of Medicine, Baltimore, Maryland, United States of America, **2** Department of Urology, Johns Hopkins University School of Medicine, Baltimore, Maryland, United States of America

* afriedm2@jhmi.edu





**Citation:** Barakat DJ, Suresh R, Barberi T, Pienta KJ, Simons BW, Friedman AD (2018) Absence of myeloid Klf4 reduces prostate cancer growth with pro-atherosclerotic activation of tumor myeloid cells and infiltration of CD8 T cells. PLoS ONE 13 (1): e0191188. https://doi.org/10.1371/journal.pone.0191188

**Editor:** Aamir Ahmad, University of South Alabama Mitchell Cancer Institute, UNITED STATES

**Received:** December 4, 2017

**Accepted:** December 29, 2017

**Published:** January 11, 2018



**Data Availability Statement:** All relevant data are within the paper and its Supporting Information files.

**Funding:** This work was supported by Department of Defense (DOD) grant PC150202, CDMRP.army.mil, and National Institutes of Health grants T32 CA60441 and P30 CA006973, www.nih.gov. The DOD grant includes funds designated for Dr. Friedman's laboratory and personnel support. The P30 grant provides Oncology enter core services.

## Abstract

The microenvironment of prostate cancer often includes abundant tumor-associated macrophages (TAMs), with their acquisition of an M2 phenotype correlating with local aggressiveness and metastasis. Tumor-derived M-CSF contributes to TAM M2 polarization, and M-CSF receptor inhibition slows prostate cancer growth in model systems. As additional cytokines can direct TAM M2 polarization, targeting downstream transcription factors could avoid resistance. Klf4 and C/EBPβ each contribute to monocyte development, and reduced expression of macrophage Klf4 or C/EBPβ favors their adoption of a pro-inflammatory M1 state. We find that a Hi-Myc C57BL/6 prostate cancer line grows more slowly in syngeneic Klf4(f/f);Lys-Cre compared with Klf4(f/f) mice when inoculated subcutaneously, but grows equally rapidly in C/EBPβ(f/f);Lys-Cre and C/EBPβ(f/f) hosts. In the absence of myeloid Klf4, TAMs have reduced expression of surface mannose receptor and *Fizz1* mRNA, both M2 markers. Global gene expression analysis further revealed activation of pro-inflammatory, pro-atherosclerotic pathways. Analysis of tumor-infiltrating lymphocytes (TILs) demonstrated markedly increased activated CD8 T cell numbers, and CD8 T cell depletion obviated the inhibitory effect of myeloid Klf4 deletion on prostate cancer growth. These findings suggest that reducing expression or activity of the Klf4 transcription factor in tumor myeloid cells may contribute to prostate cancer therapy.

## Introduction

The micro-environment of prostate cancer (PCa) often includes abundant tumor-associated macrophages (TAMs). In a study of 131 PCa patients, increased TAMs correlated with PSA >50 and increasing Gleason score or T stage. In a multivariate analysis of these data that included PSA, Gleason score, extra-capsular extension, lymph nodes metastasis, and distant

The T32 grant is a training grant which helps fund Drs. Barakat and Barberi's salaries. The Giant Food Children's Cancer Research Fund, no grant number, www.giantfood.com. Giant foods makes an annual charitable donation to our Pediatric Oncology division and the monies are used in part for maintaining laboratory equipment.

**Competing interests:** The authors have declared that no competing interests exist.

metastasis, increased TAMs was an independent poor prognostic factor for recurrence-free survival, with a hazard ratio of 2.7 [1].

Extra-cellular signals direct macrophages to a range of gene expression patterns, including the pro-inflammatory M1 and the alternatively-activated M2 states, with the majority of macrophages in a variety of established malignancies, including PCa, assuming the M2 phenotype [2–5]. Metastatic PCa lesions have increased mannose receptor (MR)-expressing M2 TAMs compared with adjacent osseous tissue [6]. Tumors resected from 93 non-metastatic PCa patients were evaluated for M1 and M2 TAM polarization. Those with extra-capsular extension (mainly Gleason 9, T3) demonstrated, on average, 4-fold more scavenger receptor expressing M2 versus scavenger receptor negative M1 TAMs, whereas organ-confined tumors (Gleason 6–7, T2) had 1.5-fold more M1 compared with M2 TAMs [7]. Moreover, in the latter study, increased M2 TAMs was associated with more rapid biochemical recurrence, in both the entire population and the subset with extra-capsular extension.

Elimination of M2 TAMs, or their conversion to the anti-tumor M1 phenotype, has therapeutic potential. Colony-stimulating factor 1 receptor (CSF1R) tyrosine kinase inhibition reduces murine PCa TAMs 15-fold, lowers expression of the *Vegfa*, *Mmp9*, and *Arg1* M2 mRNAs in the remaining TAMs, and delays tumor progression, with similar findings in immune-deficient mice inoculated with a human PCa line [8]. However, resistance to CSF1R-targeted therapy might arise via tumor secretion of alternative M2-polarizing cytokines, such as IL-4, as seen in a glioma model [9]. Targeting transcription factors that mediate M2 TAM polarization downstream of multiple cytokines might by-pass these resistance mechanisms.

Transcription factors contributing to M2 macrophage polarization include STAT6, PPARγ, NF-κB p50, Klf4, and C/EBPβ. STAT6 and PPARγ are induced by IL-4 and cooperate in M2 gene activation, while absence of the inhibitory NF-κB p50 subunit favors activation of pro-inflammatory NF-κB p65 target genes [10]. Klf4 and C/EBPβ each play a role in monocytic maturation. Increased levels of the PU.1 transcription factor favors monopoiesis over granulopoiesis and PU.1 activates *Klf4* transcription, likely in cooperation with the PU.1 partner IRF8. Klf4 rescues monopoiesis in the absence of PU.1; absence of Klf4 in marrow progenitors reduces monopoiesis, whereas exogenous Klf4 increases monopoiesis [11–15]. C/EBPβ is a leucine zipper transcription factor that binds C/EBP *cis* elements upon dimerization with another C/EBP family member; in addition, C/EBPβ zippers with AP-1 proteins such as JunB or c-Fos to bind composite DNA elements [16]. Such hybrid elements are found in regulatory regions of monocytic genes, and exogenous C/EBP:AP-1 heterodimers, but not C/EBP or AP-1 complexes alone, direct monopoiesis [17, 18].

Murine and human bone marrow-derived macrophages (BMDM) manifest reduced *Klf4* mRNA and protein in response to M1-polarizing lipopolysaccharide (LPS), whereas M2-polarizing IL-4 induces a striking increase in *Klf4* [19]. BMDM from Klf4(f/f);Lys-Cre mice, lacking myeloid Klf4 due to the lineage-restricted activity of the Lysozyme promoter, manifest reduced IL-4 induction of the *Arg1*, *MR*, *Fizz1*, and *Ym1* M2 mRNAs, and enhanced expression of the *Cox2*, *Tnfα*, and *Nos2* M1 mRNAs [19]. We find that a syngeneic Hi-Myc PCa line grows slower in Klf4(f/f);Lys-Cre compared with Klf(f/f) mice, whereas growth was not impaired in mice lacking myeloid C/EBPβ. In the absence of myeloid Klf4, TAMs had reduced expression of surface mannose receptor and *Fizz1*. Although classic M1 markers such as *Nos2* and *Tnfα* were not increased, microarray analysis revealed activation of pathways associated with pro-inflammatory states, as well as the expression of a subset of mRNAs associated with macrophage activation in atherosclerosis. In addition, tumor-infiltrating CD8 T cell numbers were markedly increased and CD8 T cell depletion obviated the slower tumor growth seen in Klf4(f/f);Lys-Cre hosts. These findings suggest that reducing expression or activity of the Klf4 transcription factor in tumor myeloid cells may contribute to prostate cancer therapy.

## Materials and methods

### Mice and ethics statement

Wild-type (WT) C57BL/6 (B6) mice were obtained from Charles River Laboratories. Lysozyme-Cre (Lys-Cre) B6 mice were obtained from Jackson Laboratory (#004781). Klf4(f/f) and C/EBPβ(f/f) B6 mice were obtained from the Mutant Mouse Regional Resource Center (#29877 and #34760). This study was carried out in strict accordance with the recommendations in the Guide for the Care and Use of Laboratory Animals of the National Institutes of Health. The protocol (M013M116) was approved by the Johns Hopkins University Animal Care and Use Committee. All efforts were made to minimize suffering. Euthanasia was carried out by carbon dioxide inhalation followed by verification of death.

### B6 Hi-Myc prostate cancer cells

After back-crossing FVB Hi-Myc mice [20] into the B6 background for >10 generations, a metastatic lesion was identified in a prostate draining lymph node from an 17-month-old mouse. Cells from this lesion were dissociated and passaged serially by subcutaneous (SQ) inoculation into the flanks of B6 mice as a B6 Hi-Myc PCa line. Hematoxylin and eosin staining of paraffin embedded tumors revealed dysplastic epithelial cells, and immunohistochemistry confirmed their expression of c-Myc and AR (S1 Fig) and CK8 (not shown). Androgen-sensitivity was confirmed by the rapid tumor regression evident upon orchiectomy (not shown).

### Tumor cell inoculation

When tumors reached 1.2–1.5 cm, mice were euthanized and tumor tissue was collected, minced with a razor blade, washed with phosphate-buffered saline (PBS), resuspended in 5mL DMEM/F12 media containing 10% FBS, 500 μL Collagenase/Hyaluronidase (Stem Cell Technologies), 2.5U/mL Dispase and 0.05mg/ml Dnase I, and then incubated at 37˚C for 1 hr with occasional mixing. Tumor tissue was vigorously triturated and passed through a 40 μM cell strainer with the aid of a syringe plunger. Cells were then pelleted at 350 g x 5 min and resuspended in PBS. Live cells were then enumerated using Trypan Blue dye and a hemocytometer, and 2E6 viable cells in 100 μL PBS were injected SQ into the shaved flank of mice anesthetized with isofluorane. Tumor growth was monitored using caliper measurements of length (L), width (W) and height (H), with volume estimated from the ellipsoid volume formula: $V = L * W * H * \pi/6$ [21]. Mice were euthanized when tumors reached 2.0 cm in largest diameter or volume greater than 1000 $mm^3$. Paraffin-embedded tumors were subjected to hematoxylin-eosin staining following by imaging at 400X using a Nikon E400 microscope, with attached CCD camera.

### T cell depletion

To deplete CD8 T cells, mice were inoculated with 200 μg rat-anti-CD8 antibody (Bio X Cell, BE0117) intraperitoneally on days -7, -5, -3 and 0 relative to Hi-Myc PCa cell inoculation (day 0). Peripheral blood obtained on d -1 from mice was subjected to flow cytometry analysis to assess depletion.

### Myeloid and T cell flow cytometry analysis

Tumors were dissociated as for cell inoculation and subjected to flow cytometry (FC) analysis, gating on live cells lacking staining with Live/Dead Aqua (ThermoFischer). All antibody staining was preceded by FcγR block on ice (eBioscience/Fisher). Extracellular antibodies were

then added and samples were incubated on ice. Intracellular staining was accomplished after surface staining using the FoxP3 staining kit (eBioscience). To evaluate myeloid subsets, total cells were stained with anti-CD11b-FITC, anti-CD45-BV650, anti-Ly6C-AF700, anti-MR-PE-Cy7, anti-CD11c-PE/Dazzle594, and anti-Ly6G-BV605 (BioLegend); anti-MHCII-eFluor450 (eBioscience); anti-CD86-PE (Miltenyi); and anti-F4/80-APC (BioRad). T cells were enumerated by staining with anti-CD45-AF700, anti-CD3-AF488, anti-CD4-PE, anti-CD8-BV655, and anti-CD69-APC-Cy7 (BioLegend), followed by intracellular stain with anti-IFNγ-APC (BioLegend). To evaluate Tregs, total cells were stained with anti-CD3-AF488, anti-CD4-BV605, and anti-CD25-PerCP-Cy5.5 (BioLegend), and then stained intracellularly with anti-FoxP3-PE (BD Pharmingen).

## RNA analysis

Tumor $CD11b^+$ cells were isolated using an anti-CD11b immunomagnetic isolation kit (Miltenyi), and RNA was isolated using NucleoSpin RNA II kit (Machery-Nagel). First-strand cDNA was prepared using AMV reverse transcriptase (Promega) and oligodT primer. Quantitative real-time PCR (qRT-PCR) was carried out using Lo-Rox SYBR Green (Alkali Scientific). Primer pairs are provided (S1 Table). For global gene expression analysis, total RNA was prepared from tumor $CD11b^+$ cells using the NucleoSpin RNA II kit. RNA quality was confirmed via Nanodrop-1000 spectrometric analysis and via a Bioanalyzer (Agilent Technologies). 500 ng total RNA from each sample was amplified and labeled using the Illumina TotalPrep RNA Amplification Kit with oligo(dT) priming (Ambion). 750 ng biotin-labeled cRNA was combined with hybridization buffer and hybridized to the Agilent Mouse GE 4 x 44K v2 Microarray at 58˚C for 16–20 hours. After hybridization, the array was washed with buffer at 55˚C and blocked at room temperature. Bound, biotinylated cRNA was stained with streptavidin-Cy3 and then washed. Dried arrays were scanned with the iScan System, and data with quantile normalization and background correction to 100 was exported from GenomeStudio v2011.1 Gene Expression Module 1.9.0 and imported to GeneSpring. Differentially expressed genes with >1.4-fold mean change were subjected to pathway analysis using Ingenuity Systems software with false discovery rate (FDR) = 0.05 as threshold.

## Immunohistochemistry

Immunohistochemistry was performed as previously described [22]. Briefly, heat-induced antigen retrieval was carried out in a steam chamber followed by washing in Tris-buffered saline. Endogenous peroxidases were inactivated with Bloxall (Vector labs), and sections were blocked with Dako blocking buffer (Agilent Technologies), incubated with primary antibodies (anti-c-Myc, anti-AR), washed, and then incubated with horse radish peroxidase-conjugated secondary antibodies. Chromagen was developed with DAB solution (Vector Labs) and counterstained with Meyer's hematoxylin. Primary antibodies used were anti-cMyc (Abcam, clone 769, 1:1000), anti-Androgen Receptor (Santa Cruz, clone N-20, 1:500), and anti-CK8 (Covance, clone 1E8, 1:1000).

## Statistics

Tumor volumes, tumor growth rates, myeloid and T cell subsets, and RNA expression values were compared using the Student *t* test. Tumor growth rates were estimated by fitting exponential curves to volume data (Excel) for each tumor according to the equation $V = V_o e^{bt}$ (V = volume, $V_o$ = initial volume, t = time in days and b = exponential slope). The slope or growth rate was estimated as the value 'b' from the above equation because $\ln(V) = \ln(V_o) + bt$. Means and standard errors (SE) are shown.

## Results

### Hi-Myc prostate cancer growth is slowed in the absence of myeloid Klf4

*Klf4* mRNA was reduced 11-fold in Klf4(f/f);Lys-Cre compared with Klf4(f/f) peritoneal macrophages (S2A Fig), consistent with prior findings with this model [19]. B6 Hi-Myc PCa cells were inoculated into the flanks of B6 Klf4(f/f) and Klf4(f/f);Lys-Cre mice and tumor volumes were monitored every 2–3 days beginning on day 22 (Fig 1A). Initial growth was uniformly slower in the absence of myeloid Klf4, with mean tumor volumes on day 29, with 6.4-fold lower mean tumor volumes in the Klf4(f/f);Lys-Cre recipients (Fig 1B). Plotting the estimated tumor volumes subsequent to day 22 on a logarithmic scale allows fitting later growth rates to best fit lines (Fig 1C), with the slopes of these lines on average ~2-fold lower in the Klf4(f/f);Lys-Cre cohort (Fig 1D). The average, estimated growth rates predict a 7-fold difference in tumor volume on day 29, similar to what was found by caliper measurements. In additional mice sacrificed on days 24–29 for tumor myeloid or T cell analyses, the tumor volumes were also significantly lower in the absence of myeloid Klf4 (S3 Fig).

### Hi-Myc prostate cancer has increased TAMs with reduced MR and increased CD11c in the absence of myeloid Klf4

To evaluate how Klf4 influences myeloid composition and macrophage polarization in Hi-Myc tumors, we analyzed a panel of surface markers on dissociated tumor cells by multi-color flow cytometry (Fig 2A). $CD45^{+}CD11b^{+}$ myeloid cells represented ~20% of live tumor cells

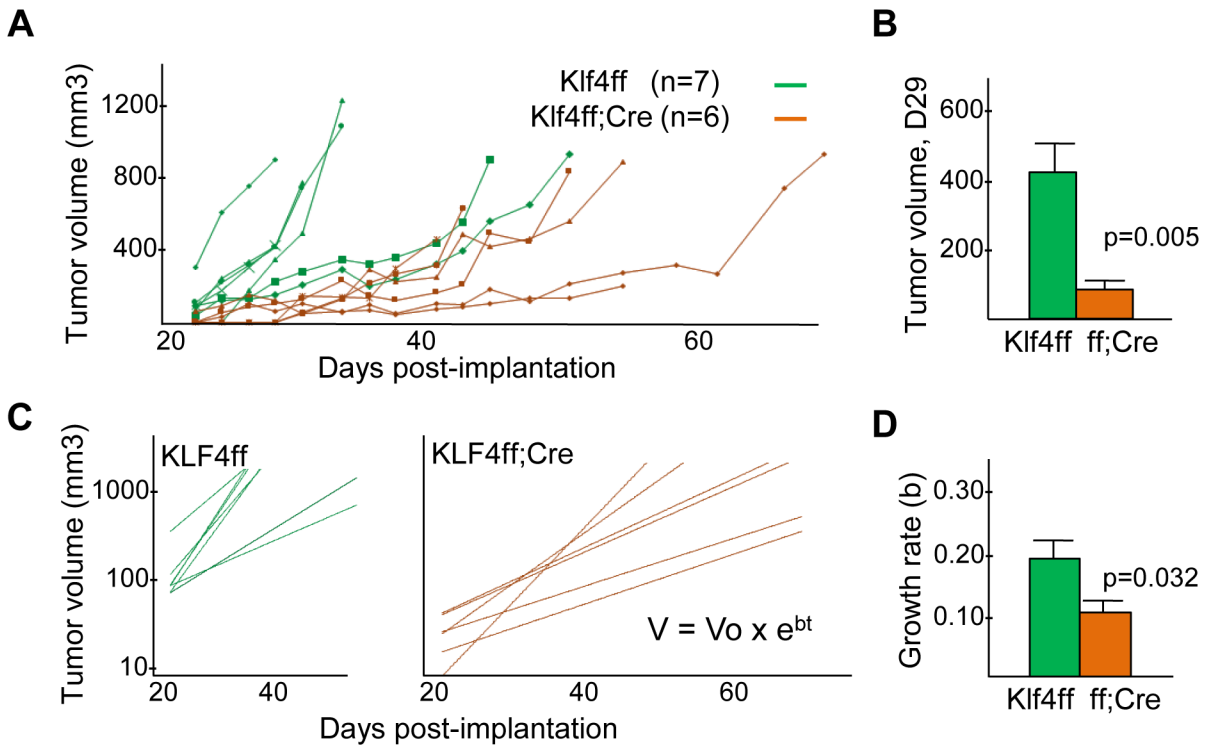


**Fig 1. Hi-Myc prostate cancer grows more slowly in the absence of myeloid Klf4. A)** Estimated tumor volumes evaluated every 2–3 days after inoculation of B6 Hi-Myc tumor cells SQ into the flanks of Klf4(f/f) or Klf4(f/f);Lys-Cre mice. **B)** Estimated day 29 tumor volumes (~Vo) (mean and SE). **C)** Best fit lines of estimated tumor volumes versus time, $V = Vo + e^{bt}$ for these same data. **D)** Mean exponential gowth rates, "b", of Hi-Myc tumors (mean and SE).

https://doi.org/10.1371/journal.pone.0191188.g001

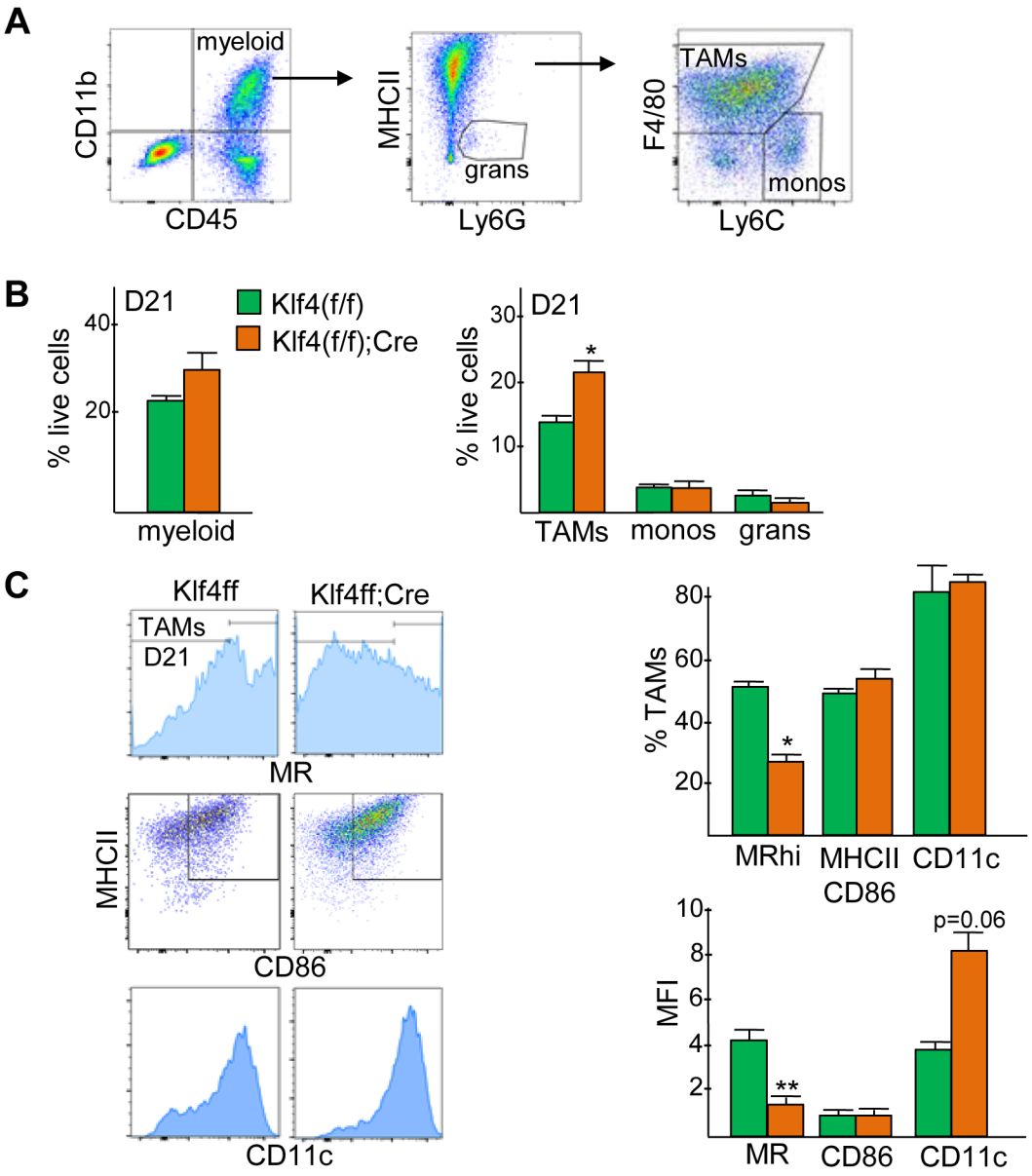


**Fig 2. Hi-Myc prostate cancer increases TAMs with reduced mannose receptor in the absence of myeloid Klf4. A)** Gating strategy for identifying $CD45^{+}CD11b^{+}$ tumor myeloid cells, and TAMs, monocytes, and granulocytes within the tumor myeloid population. **B)** Quantification of myeloid cells (left) and myeloid subsets (right) as a percentage of viable tumor cells in Klf4(f/f) and Klf4(f/f);Lys-Cre PCa recipients 21 days after inoculation of Hi-Myc PCa (mean and SE, n = 3). **C)** Representative FC plots (left) for MR, MHCII;CD86 and CD11c expression, bar graphs (right) showing the percentage of $MR^{hi}$, $MHCII^{+}CD86^{+}$, and $CD11c^{+}$ TAMs (top), and the mean fluorescence intensity (MFI) in these populations (bottom) on day 21 in Klf4(f/f) and Klf4(f/f);Lys-Cre PCa recipients (mean and SE, n = 3). $^{*}$ $p < 0.05$, $^{**}$ $p < 0.01$, $^{***}$ $p < 0.001$.

https://doi.org/10.1371/journal.pone.0191188.g002

isolated on day 21 from Klf4(f/f) and ~29% of Klf4(f/f);Lys-Cre Hi-Myc PCa recipients, p = 0.07 (Fig 2B, right). The majority of tumor myeloid cells were $F4/80^{hi}Ly6C^{lo/mid}$ TAMs, and these increased approximately 1.5-fold in the absence of myeloid Klf4 (Fig 2B, left). The day 21 TAM population was further characterized by analysis of surface MR, MHCII/CD86, and CD11c (Fig 2C). $MR^{hi}$ cells, representing M2-biased TAMs, were reduced 1.8-fold, and $MHCII^{+}CD86^{+}$ cells, representing M1-biased TAMs, were unchanged. The mean fluorescence

intensity (MFI) of CD11c, present on activated macrophages [23], was increased 2-fold in Klf4 (f/f);Lys-Cre compared with Klf4(f/f) PCa tumor recipients. These data demonstrate that myeloid Klf4 promotes an M2 TAM phenotype in Myc-driven prostate cancer.

## Hi-Myc prostate cancer growth and tumor myeloid cells are unaffected by absence of myeloid C/EBPβ

C/EBPβ is another transcription factor reported to promote M2 polarization [10]. To test whether tumor myeloid cells utilize C/EBPβ to drive an M2 phenotype in prostate cancer, we evaluated Hi-Myc tumors in C/EBPβ(f/f) and C/EBPβ(f/f);Lys-Cre mice. C/EBPβ mRNA was reduced >100-fold in C/EBPβ(f/f);Lys-Cre compared with C/EBPβ(f/f) peritoneal macrophages (S2B Fig). Hi-Myc PCa cells were inoculated into the flanks of B6 C/EBPβ(f/f) and C/EBPβ(f/f);Lys-Cre mice and tumor volumes were monitored every 2–3 days beginning on d21. Tumor growth rates were similar in the two cohorts (Fig 3A). Tumor cell FC analysis found no differences in the proportions of total myeloid cells, TAMs, monocytes, granulocytes, $MR^{hi}$ TAMs, or $MHCII^{+}CD86^{+}$ TAMs on day 21 in control or C/EBPβ-deleted prostate cancer recipients (Fig 3B). Neither the proportion of TAMs expressing CD11c nor their CD11c MFI was affected by absence of C/EBPβ (not shown). These data demonstrate that myeloid expression of C/EBPβ does not affect TAM polarization or Hi-Myc tumor growth.

## Hi-Myc prostate cancer myeloid cells lacking Klf4 express RNAs associated with pro-inflammatory pathways

$CD11b^{+}$ myeloid cells were isolated from Hi-Myc prostate cancers 21 days after inoculation into Klf4(f/f) or Klf4(f/f);Lys-Cre recipients. RNA from these cells was analyzed for a panel of M1 and M2 macrophage markers by qRT-PCR (Fig 4). Most were not significantly changed, though the M1 marker *Ccl2* was increased and the M2 marker *Fizz1* decreased in the absence of myeloid Klf4. *IL-1b* and *IL-6* were also not significantly different between the two groups (not shown). Consistent with our findings with peritoneal macrophages, TAM *Klf4* mRNA was reduced 10-fold in the presence of Lys-Cre (S4 Fig).

To further evaluate the influence of Klf4 on TAM polarization, RNAs isolated from $CD11b^{+}$ tumor myeloid cells from two tumors in each host were subjected to global gene expression analysis. mRNAs corresponding to 277 genes were up-regulated and 119 down-regulated 1.4-fold or greater in the absence of myeloid Klf4 (S2 Table). Ingenuity Pathway analysis revealed activation of pathways involved in cellular movement, inflammation and adhesion. Genes increased or decreased within these pathways in our data set are listed (Table 1). Because "Atherosclerosis Signaling" was the top regulated pathway from our analysis we compared our microarray data to a recent proteomic analysis of atherosclerotic plaques from human patients that underwent endarterectomy [24]. 20 genes that were differentially regulated in $CD11b^{+}$ cells overlapped with 146 extracellular matrix (ECM) or ECM-related proteins identified in atherogenic plaques. Of these 20 genes, 19 were upregulated in tumors that formed in Lys-Cre;Klf4(f/f) mice (Table 2). These results suggest that myeloid deletion of Klf4 promotes an atherogenic-like microenvironment in Hi-Myc prostate cancer.

## Absence of myeloid Klf4 increases activated $CD8^{+}$ T-cells in Hi-Myc prostate cancer

Induction of pro-inflammatory pathways in tumor myeloid cells by Klf4 deletion might induce immune cell influx and activation. Prostate cancers from Klf4(f/f) or Klf4(f/f);Lys-Cre mice were analyzed for CD3, CD4 and CD8 tumor-infiltrating lymphocytes (TIL) on day 21

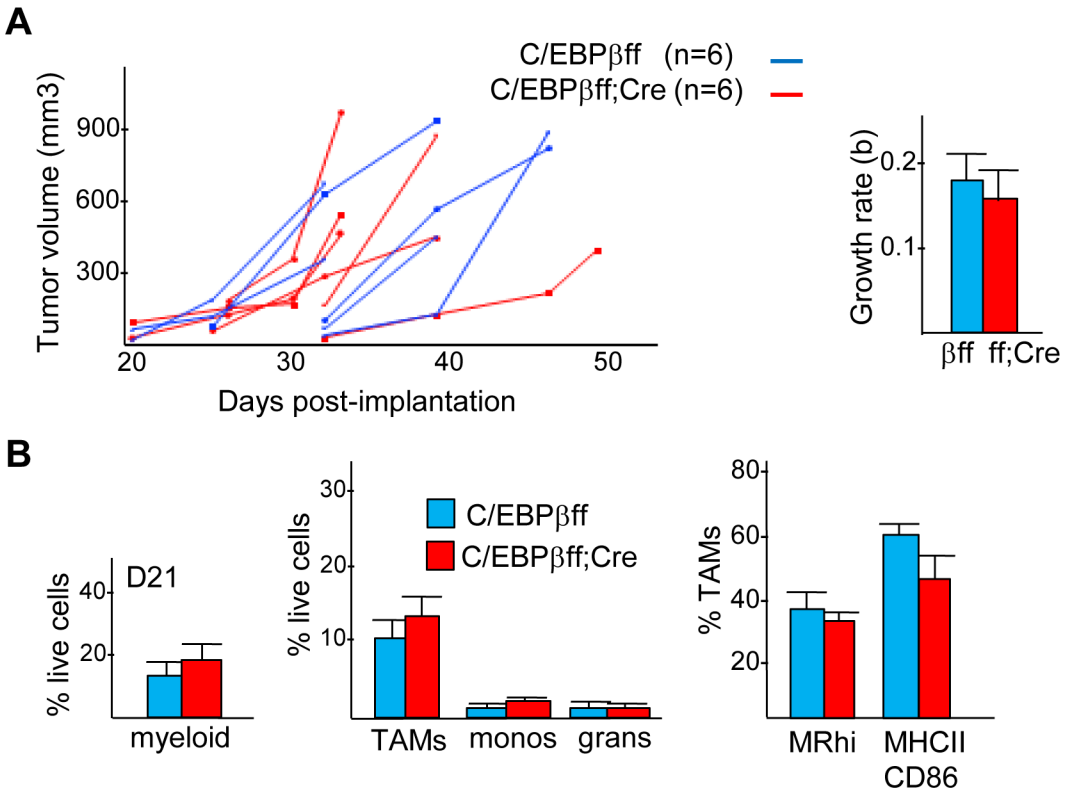


**Fig 3. Absence of myeloid C/EBPβ does not affect growth of Hi-Myc prostate cancer. A)** Estimated tumor volumes evaluated every 2–3 days after inoculation of B6 Hi-Myc PCa cells SQ into the flanks of C/EBPβ(f/f) or C/EBPβ(f/f);Lys-Cre mice. **B)** Percentage of myeloid cells, TAMs, monocytes, and granulocytes amongst viable tumor cells on day 21 (mean and SE, n = 3).

https://doi.org/10.1371/journal.pone.0191188.g003

(Fig 5A). $CD3^+$ cells, representing total T cells, were increased 2-fold, and CD8 TIL were increased 4-fold in the absence of myeloid Klf4, whereas CD4 T cell numbers were unchanged. In absolute terms, CD8 T cells represented ~8% of viable tumor cells. Activation of CD8 T cells was assessed by staining for intracellular IFNγ or surface CD69 (Fig 5B). The frequency of CD8 T cells expressing these markers were markedly increased in Klf4(f/f);Lys-Cre hosts, representing 1.5% or 3% of viable tumor cells. The proportion of $CD3^+CD4^+CD25^+Foxp3^+$ Tregs was not changed (Fig 5C), indicating an overall increase in the CD8:Treg ratio.

To determine the contribution of CD8 T cells to the slower growth of Hi-Myc PCa calls in Klf4(f/f);Lys-Cre mice, we used antibody to deplete CD8 T cells. Klf4(f/f) and Klf4(f/f);Lys-Cre mice received 4 doses of CD8 antibody 7, 5, 3 and 0 days prior to PCa cell implantation, and depletion was confirmed by FC analysis of peripheral blood 1 day prior to implantation (Fig 6A and 6B). Hi-Myc PCa growth rates were similar in both cohorts (Fig 6C–6E). Thus, CD8 depletion eliminated the difference in growth rates between Hi-Myc tumors grown in Klf4 (f/f) and Klf4(f/f); Lys-Cre mice shown in Fig 1. These results suggest that CD8 T cells are critical for suppressing Hi-Myc prostate tumor growth in Klf4(f/f); Lys-Cre mice.

## Discussion

Klf4 and C/EBPβ are transcription factors that play a role in monocyte development and favor macrophage M2 polarization. The Lys-Cre transgene deletes floxed alleles in macrophages, activated monocytes, and granulocytes [25]. We found that B6 Hi-Myc PCa tumors grew more

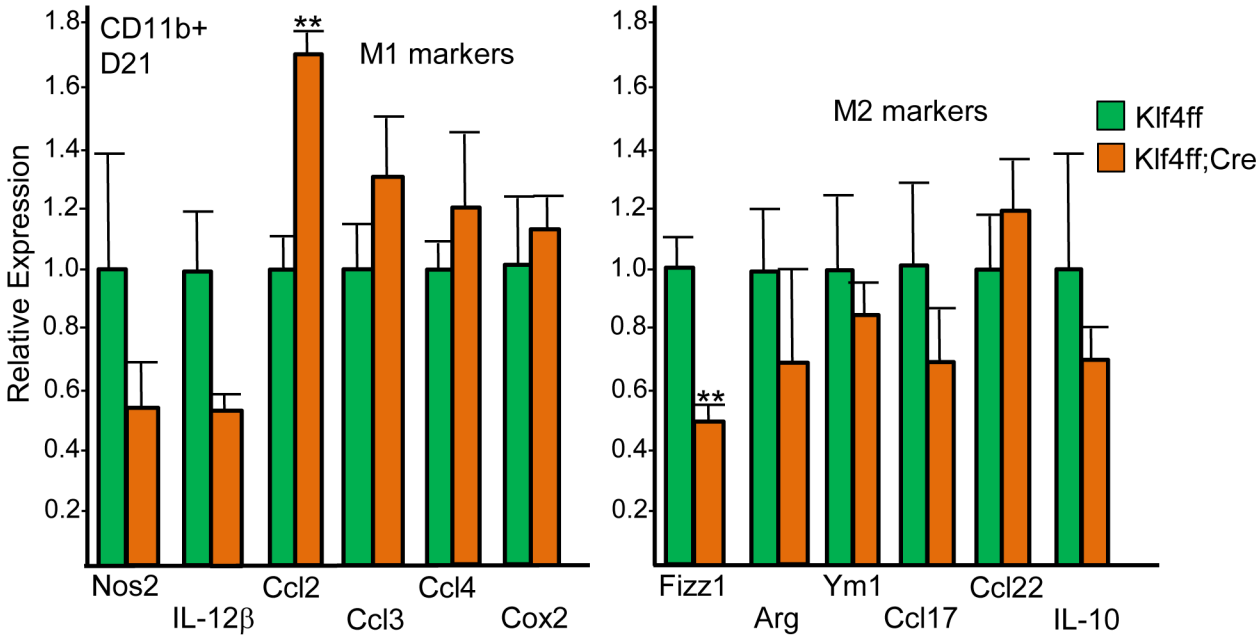


**Fig 4. Expression of a subset of M1 and M2 mRNAs in Hi-Myc prostate cancer myeloid cells in Klf4(f/f) versus Klf4(f/f);Lys-Cre hosts.** RNAs prepared from tumor CD11b$^+$ cells on day 21 after Hi-Myc PCa inoculation were subjected to quantitative RT-PCR analysis for the indicated M1 and M2 markers and for the RNA encoding *cyclophilin A* as an internal control. The relative expression of each mRNA is shown for Klf4(f/f) and Klf4(f/f);Lys-Cre recipients, with expression in Klf4(f/f) mice set to 1.0 (mean and SE, n = 5).

https://doi.org/10.1371/journal.pone.0191188.g004

**Table 1. Ingenuity pathway analysis of Klf4(f/f) vs Klf4(f/f);Lys-Cre PCa myeloid cells*.**

| Pathway (-logB-H p-value) | RNAs higher in Klf4(f/f);Lys-Cre | RNAs higher in Klf4(f/f) |
|---|---|---|
| Atherosclerosis Signaling (5.01) | Mmp3, CD36, Clu, Cma1, Col1a1, Col1a2, Col3a1, IL1rn, Rbp4, S100a8 | Lyz, Pdgfb, Tnf |
| LXR/RXR Activation (4.56) | Ahsg, CD36, Clu, IL1r2, IL1rn, Lbp, Rbp4, Vtn, S100a8 | Lyz, Nos2,Tnf |
| Granulocyte Adhesion and Diapedesis (3.98) | Ccl7, Cldn3, Cldn10, Fpr1, Hspb1 IL1r2, IL1rn, Mmp3, Pf4, Sell | Ccl24,Cxcl9,Tnf |
| Agranulocyte Adhesion and Diapedesis (3.79) | Acta2, Ccl7, Cldn3, Cldn10, IL1rn, Mmp3, Myl9, Pf4, Sell | Ccl24, Cxcl9, Fn1, Tnf |
| Hepatic Fibrosis/Hepatic Stellate Cell Activation (3.52) | Acta2, Ccr7, Col1a1, Col1a2, Col3a1, Igfbp5, IL1r2, Lbp, Myl9 | Fn1, Pdgfb, Tnf |
| Acute Phase Response Signaling (2.67) | Ahsg, C1r, Hp, IL1rn, Lbp, Rbp1, Rbp4, Saa3, Serping1 | Fn1, Tnf |
| Altered T Cell and B Cell Signaling in Rheumatoid Arthritis (RA) (2.67) | Spp1, IL1rn | HLA-DMA, HLA-DQA1, HLA-DRB5, Tlr12, Tnf, Tnfsf13b |
| Role of Macrophages, Fibroblasts and Endothelial Cells in RA (2.49) | Dkk3, IL1r2, IL1rn, Mmp3, Sfrp2, Traf4 | Camk2d, Cebpe, Fn1, Nos2, Pdgfb, Prkcb, Tlr12, Tnf, Tnfsf13b |
| T Helper Cell Differentiation (2.49) | | Icosl, IL2ra, HLA-DMA, HLA-DQA1, HLA-DRB5, Tgfbr1, Tnf |
| Communication Between Innate and Adaptive Immune Cells (2.46) | Ccr7, IL1rn | HLA-DRB5, Ifnb1 Tlr12, Tnf, Tnfsf13b |

*Top 10 Ingenuity Pathways comparing mean RNA levels from CD11b$^+$ myeloid cells isolated from Hi-Myc PCa tumors in Klf4(f/f) vs Klf4(f/f)Lys-Cre hosts (n = 2 per group).

https://doi.org/10.1371/journal.pone.0191188.t001

**Table 2. Extracellular atherosclerosis plaque proteins in myeloid cells lacking Klf4*.**

| RNAs higher in Klf4(f/f);Lys-Cre | RNAs higher in Klf4 (f/f) |
|---|---|
| Aebp1, Clu, Col1a1, Col3a1, Cpa3, Dcn, Htra1, Lama5, Lamb2, Lum, Mfge8, Pcolce, S100a8, S100a9, Saa3, Serping1, Spp1, Tnxb, Vtn | Fn1 |

*RNAs increased or reduced >1.4-fold that correspond to extracellular proteins in carotid plaques but not in normal carotid arteries.

https://doi.org/10.1371/journal.pone.0191188.t002

slowly when inoculated subcutaneously in Klf4(f/f);Lys-Cre compared with Klf4(f/f) hosts, both during the first 21–29 days when tumors become detectable and thereafter. In contrast, there was no difference in Hi-Myc PCa growth kinetics in C/EBPβ(f/f);Lys-Cre versus C/EBPβ (f/f) recipients. Limitations of our study include lack of evaluation in the orthotopic prostate environment, which can be challenging due to early ureteral obstruction and difficulty with monitoring tumor growth, and lack of evaluation of the effects of myeloid KLF4 deletion using additional prostate cancer models.

Amongst tumor myeloid cells, TAMs predominated over monocytes and granulocytes in this model, and F4/80$^+$ TAMs were increased 2-fold in the absence of Klf4. TAMs lacking Klf4 manifested substantial reduction in surface MR and *Fizz1* mRNA expression (M2 markers) and a gene expression signature demonstrating activation of multiple pro-inflammatory pathways. CD11b$^+$ cells from tumors grown in Klf4(f/f);Lys-Cre mice displayed increased expression of several interferon-regulated genes (*Ifi27l2a*, *Isg20*, *Oasl1*, *Irf7* and *Mx2*), indicating an activated innate immune cell phenotype. However, several classic M1 genes, including *Ifnb*, *Tnf*, *Cxcl9*, and genes encoding MHC II subunits showed higher expression in Klf4(f/f) control mice. This suggests that deletion of Klf4 influences specific aspects of M1 differentiation and represses others in the Hi-Myc PCa microenvironment and perhaps less than that seen upon culture of Klf4(f/f) versus Klf4(f/f);Lys-Cre BMDM in IFNγ (M1 inducer) or IL-4 (M2 inducer) [19].

Notably, "Atherosclerosis Signaling" was the top pathway associated with the gene expression pattern in Klf4-deleted CD11b$^+$ myeloid cells isolated from Hi-Myc tumors. Atherosclerosis is a progressive disease that narrows the vascular lumen through a buildup of arterial plaque, an amalgam of lipids, macrophages and other leukocytes, smooth muscle cells, endothelial cells (EC), necrotic regions, and extracellular proteins. Nascent atherosclerotic plaques activate the vascular endothelium by increasing shear stress and by releasing pro-inflammatory cytokines, promoting recruitment and invasion of monocytes and other blood cells [26,27]. Klf4 has been identified as a critical molecule involved in the pathogenesis of atherosclerosis in macrophages and ECs. Exposure of peritoneal macrophages to an inflammatory lipid reduces Klf4 and increases M1 mRNAs, the latter induced to a greater extent in Klf4(f/f);Lys-Cre macrophage, and absence of myeloid Klf4 augments atherosclerosis in ApoE-/- mice [28]. Exposure of ECs to pro-inflammatory cytokines or shear stress reduces their expression of Klf4, deletion of endothelial Klf4 augments atherosclerosis, and transgenic EC-Klf4 reduces atherosclerosis [29,30]. Notably, we found that 20 differentially regulated genes from our microarray analysis matched proteomic analysis of extracellular proteins from atherosclerotic plaques [24], with a striking 19 out of these 20 mRNAs having higher expression in myeloid cells obtained from prostate cancers growing in Lys-Cre;Klf4(f/f) compared with the Klf4(f/f) hosts.

In addition, we observed a nearly 2-fold increase in the frequency of tumor CD3$^+$ T cells and a 4-fold increase in tumor CD8$^+$ T cells in response to myeloid Klf4 deletion. Amongst

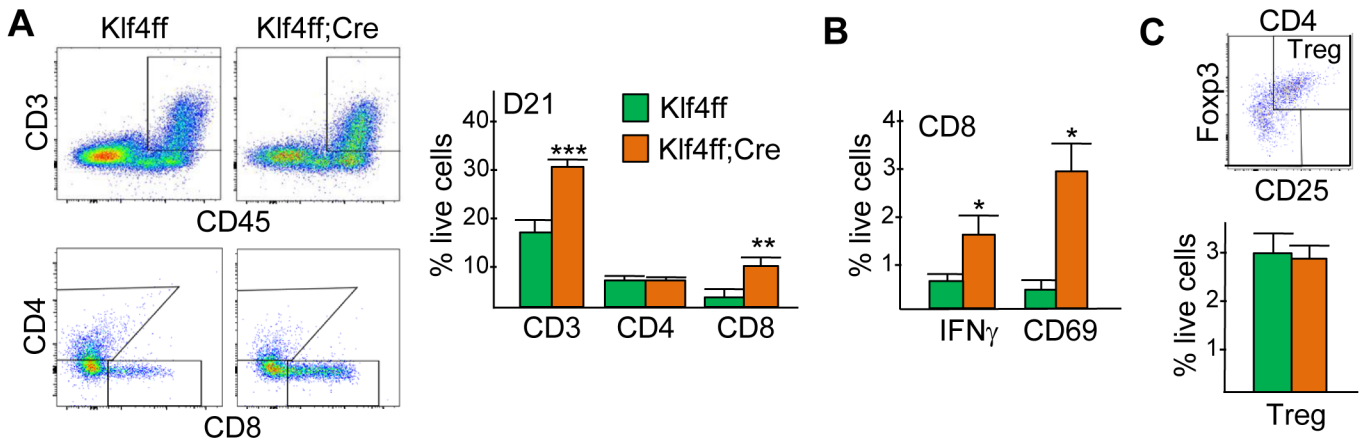


**Fig 5. Increased number of activated CD8 T cells in Hi-Myc prostate cancer in hosts lacking myeloid Klf4. A)** Representative FC plots for CD45;CD3 expression and for CD4 and CD8 expression amongst $CD45^+CD3^+$ tumor cells (left) and the percentage of CD3, CD4, or CD8 T cells amongst viable tumor cells on day 21 in Klf4(f/f) and Klf4(f/f);Lys-Cre Hi-Myc PCa recipients (right, mean and SE, n = 3). **B)** Percentage of $CD45^+CD3^+CD8^+IFN\gamma^+$ or $CD45^+CD3^+CD8^+CD69^+$ cells amongst live tumor cells on d21. **C)** Percentage $CD3^+CD4^+CD25^+Foxp3^+$ Treg cells on day 21 in Klf4(f/f) and Klf4(f/f);Lys-Cre PCa recipients (right, mean and SE, n = 3).

https://doi.org/10.1371/journal.pone.0191188.g005

CD8 T-cells, there was no change in the percentage of cells expressing IFNγ or CD69, indicating that myeloid Klf4 deletion did not augment CD8 lymphocyte activation. We found that CD8 T cells were critical for the growth defect caused by absence of myeloid Klf4 because depletion of CD8 T cells eliminated the growth deficit observed in Hi-Myc tumors. As Treg numbers were unchanged, the CD8 effector:Treg ratio was similarly increased. Notably, the CD8:Treg ratio has been shown to correlate with favorable prognosis in prostate cancer [31,32]. Cxcl9, a widely reported T-cell chemoattractant, was down-regulated in Klf4(f/f);Lys-Cre mice and our data did not reveal up-regulation of genes involved in T cell chemotaxis. These findings suggest that upregulation of chemokines is not likely to explain the rise in tumor T cell frequency in the Klf4(f/f);Lys-Cre mice. In co-cultures of Klf4(f/f) or Klf4(f/f);Lys-Cre $CD11b^+$ tumor cells with splenic T cells stimulated with anti-CD3 and anti-CD28, we did not observe a difference in CD8 T cell proliferation (not shown), suggesting that increased proliferation also does not explain the observed increase in T cell frequency.

Increased T cell numbers in Hi-Myc tumors forming in Klf4(f/f);Lys-Cre mice is potentially related to a change in the composition of the ECM generated by $CD11b^+$ tumor myeloid cells lacking Klf4. The expression of $\alpha_5$, $\beta_1$ and $\beta_3$ integrins promotes retention and motility of activated T cells in inflamed non-lymphoid tissues dependent upon binding to fibronectin and collagenous fibers of the ECM [33–36]. In atherosclerotic lesions, T cells accumulate within the fibrous cap, where the ECM is composed of types I and III collagen with small patches of fibronectin [37]. CD8 T cells enter the arterial wall of atherogenic plaques and represent the dominant lymphocyte during advanced, high risk plaques, which coincides with active degradation of the plaque ECM by infiltrating macrophages [38,39]. We observed an increase in types I and III collagen, *Pcolce* (a collagen endopeptidase required for maturation of pro-collagen), and *Dcn* (a proteoglycan involved in the staggered assembly of collagen molecules in myeloid cells from Klf4(f/f);Lys-Cre vs Klf4(f/f) tumors. Low density ECM has the potential to suppress tumorigenicity via T cell recruitment; for example, in explants from human lung tumors and lung tumor xenografts T cells are motile along low density ECM fibers and excluded from areas of high ECM density [40,41]. Interestingly, myeloid *Fizz1/Relmα* expression, which was substantially decreased in Klf4(f/f);Lys-Cre tumor myeloid cells, was shown to

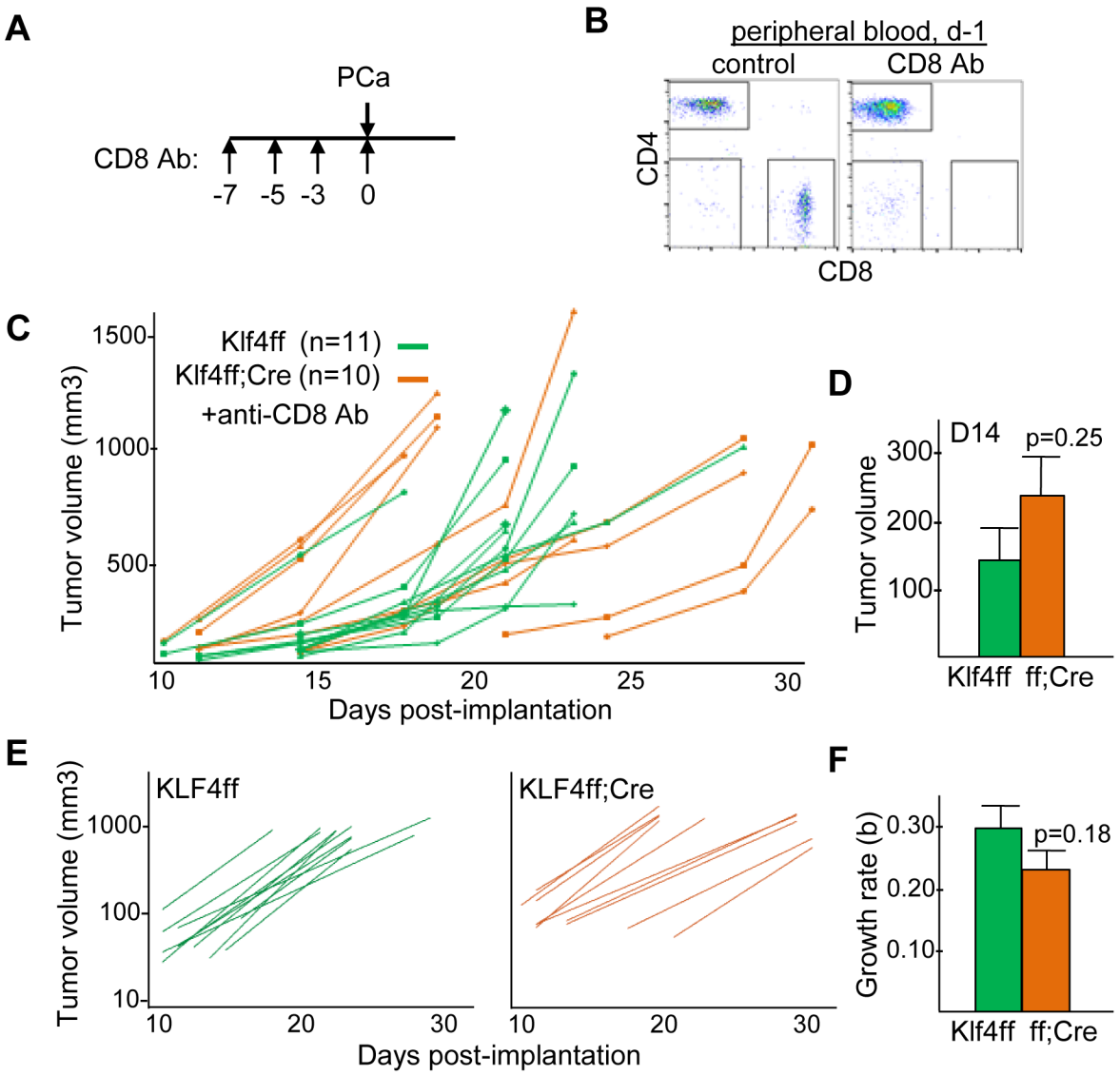


**Fig 6. CD8 T cell depletion eliminates slower growth of Hi-Myc prostate cancer in mice lacking myeloid Klf4. A)** Klf4(f/f) and Klf4(f/f);Lys-Cre mice received CD8 antibody (Ab) on days -7, -5, -3, and 0 followed by Hi-Myc PCa cell inoculation on d0, as diagrammed. **B)** Representative CD4;CD8 FACS plots demonstrating efficient depletion of CD8 T cells from the peripheral blood one day prior to PCa inoculation **C)** Estimated tumor volumes evaluated every 2–3 days after inoculation. **D)** Estimated day 14 tumor volumes, Vo (mean and SE). **E)** Best fit lines for the estimated tumor volumes versus time, $V = Vo + e^{bt}$ for these same data. **F)** Mean exponential growth rates, "b", of Hi-Myc tumors (mean and SE).

https://doi.org/10.1371/journal.pone.0191188.g006

promote collagen-cross linking, increase collagen fibril density and facilitate wound healing in a model of cutaneous injury [42], further suggesting presence of low-density collagen fibers in Hi-Myc PCa tumors in Klf4(f/f);Lys-Cre recipients.

In conclusion, our findings implicate myeloid Klf4 in prostate cancer progression. Targeting myeloid Klf4 may provide therapeutic benefit to PCa patients via induction of a pro-inflammatory myeloid program and increased density of activated CD8 T cells and CD8:Treg ratio, potentially through effects on macrophage-mediated ECM remodeling.

## Supporting information

**S1 Fig. Hi-Myc prostate cancer cells.** A tumor grown subcutaneously in a WT host was fixed, paraffin-embedded, sectioned, and subjected to hematoxylin-eosin (H/E) staining or to immunohistochemistry for c-Myc or androgen receptor (AR). Images shown are 60X.
(TIF)

**S2 Fig. Markedly reduced expression of floxed *Klf4* or *Cebpb* in macrophages mediated by Lys-Cre. A)** RNA isolated from peritoneal macrophages from Klf4(f/f) or Klf4(f/f);Lys-Cre mice were subjected to quantitative RT-PCR for Klf4 relative to *cyclophilin A* (n = 2/group) **B)** RNA isolated from peritoneal macrophages from C/EBPβ(f/f) or C/EBPβ(f/f);Lys-Cre mice were subjected to quantitative RT-PCR for *Cebpb* relative to *cyclophilin A* (n = 2/group).
(TIF)

**S3 Fig. Absence of myeloid Klf4 reduces Hi-Myc prostate cancer tumor volumes in additional recipients.** Tumor volumes assessed at the time of sacrifice of mice used for tumor myeloid or T cell analysis are shown after inoculation into Klf4(f/f) or Klf4(f/f);Lys-Cre recipients.
(TIF)

**S4 Fig. Marked reduction of Klf4 in Hi-Myc prostate cancer tumors in Klf4(f/f);Lys-Cre mice.** RNAs prepared from tumor $CD11b^+$ cells on day 21 after Hi-Myc PCa inoculation were subjected to quantitative RT-PCR analysis for *Klf4* and for the RNA encoding *cyclophilin A* as an internal control.
(TIF)

**S1 Table. Primers used for quantitative RT-PCR.**
(DOCX)

**S2 Table. RNAs whose expression was changed >1.4-fold by myeloid Klf4 deletion in $CD11b^+$ prostate cancer tumor cells.**
(XLSX)

## Acknowledgments

We thank Wayne Yu for his assistance with analysis of microarray data.

## Author Contributions

**Conceptualization:** David J. Barakat, Kenneth J. Pienta, Brian W. Simons, Alan D. Friedman.

**Formal analysis:** David J. Barakat.

**Funding acquisition:** Kenneth J. Pienta, Alan D. Friedman.

**Investigation:** David J. Barakat, Rahul Suresh, Theresa Barberi, Brian W. Simons, Alan D. Friedman.

**Methodology:** Brian W. Simons.

**Supervision:** Kenneth J. Pienta, Brian W. Simons, Alan D. Friedman.

**Writing – original draft:** Alan D. Friedman.

**Writing – review & editing:** David J. Barakat, Rahul Suresh, Theresa Barberi, Kenneth J. Pienta, Brian W. Simons.

## References


1. Nonomura N, Takayama H, Nakayama M, Nakai Y, Kawashima A, Mukai M, et al. Infiltration of tumour-associated macrophages in prostate biopsy specimens is predictive of disease progression after hormonal therapy for prostate cancer. BJU International 2011; 107: 1918–1922. https://doi.org/10.1111/j.1464-410X.2010.09804.x PMID: 21044246
2. Sica A, Bronte V. Altered macrophage differentiation and immune dysfunction in tumor development. J Clin Invest. 2007; 117: 1155–1166. https://doi.org/10.1172/JCI31422 PMID: 17476345
3. Mosser DM, Edwards JP. Exploring the full spectrum of macrophage activation. Nat Rev Immunol. 2008; 8: 858–869.
4. Franklin RA, Liao W, Sarkar A, Kim MV, Bivona MR, Liu K, et al. The cellular and molecular origin of tumor-associated macrophages. Science 2014; 344: 921–925. https://doi.org/10.1126/science.1252510 PMID: 24812208
5. Noy R, Pollard JW. Tumor-associated macrophages: from mechanisms to therapy. Immunity 2014; 41: 49–61. https://doi.org/10.1016/j.immuni.2014.06.010 PMID: 25035953
6. Roca H, Varsos ZS, Sud S, Craig MJ, Ying C, Pienta KJ. CCL2 and interleukin-6 promote survival of human CD11b$^+$ peripheral blood mononuclear cells and induce M2-type macrophage polarization. J Biol Chem. 2009; 284: 34342–34354. https://doi.org/10.1074/jbc.M109.042671 PMID: 19833726
7. Comito G, Giannoni E, Segura CP, Barcellos de Souza P, Raspollini MR, Baroni G, et al. Cancer-associated fibroblasts and M2-polarized macrophages synergize during prostate carcinoma progression. Oncogene 2014; 33: 2423–2431. https://doi.org/10.1038/onc.2013.191 PMID: 23728338
8. Escamilla J, Schokrpur S, Liu C, Priceman SJ, Moughon D, Jiang Z, et al. CSF1 receptor targeting in prostate cancer reverses macrophage-mediated resistance to androgen blockade therapy. Cancer Res. 2015; 5: 950–962.
9. Quail DF, Bowman RL, Akkari L, Quick ML, Schuhmacher AJ, Huse JT, et al. The tumor microenvironment underlies acquired resistance to CSF-1R inhibition in gliomas. Science 2016; 352: aad3018. https://doi.org/10.1126/science.aad3018 PMID: 27199435
10. Tugal D, Liao X, Jain MK. Transcriptional control of macrophage polarization. Arterioscler Thromb Vasc Biol. 2013; 33: 1135–1144. https://doi.org/10.1161/ATVBAHA.113.301453 PMID: 23640482
11. Dahl R, Walsh JC, Lancki D, Laslo P, Iyer SR, Singh H, et al. Regulation of macrophage and neutrophil cell fates by the PU.1:C/EBPα ratio and granulocyte colony-stimulating factor. Nat Immunol. 2003; 4: 1029–1036. https://doi.org/10.1038/ni973 PMID: 12958595
12. Rosenbauer F, Wagner K, Kutok JL, Iwasaki H, Le Beau MM, Okuno Y, et al. Acute myeloid leukemia induced by graded reduction of a lineage-specific transcription factor, PU.1. Nat Genet. 2004; 36: 624–630. https://doi.org/10.1038/ng1361 PMID: 15146183
13. Dakic A, Metcalf D, Di Rago L, Mifsud S, Wu L, Nutt SL. PU.1 regulates the commitment of adult hematopoietic progenitors and restricts granulopoiesis. J Exp Med. 2005; 201: 1487–1502. https://doi.org/10.1084/jem.20050075 PMID: 15867096
14. Feinberg MW, Wara AK, Cao Z, Lebedeva MA, Rosenbauer F, Iwasaki H, et al. The Kruppel-like factor KLF4 is a critical regulator of monocyte differentiation. EMBO J. 2007; 26: 4138–4148. https://doi.org/10.1038/sj.emboj.7601824 PMID: 17762869
15. Kurotaki D, Osato N, Nishiyama A, Yamamoto M, Ban T, Sato H, et al. Essential role of the IRF8-KLF4 transcription factor cascade in murine monocyte differentiation. Blood 2013; 121: 1839–1849. https://doi.org/10.1182/blood-2012-06-437863 PMID: 23319570
16. Hong SH, Skaist AM, Wheelan SJ, Friedman AD. AP-1 protein induction during monopoiesis favors C/EBP:AP-1 heterodimers over C/EBP homodimerization and stimulates FosB transcription. J Leuk Biol. 2011; 90: 643–651.
17. Cai DH, Wang D, Keefer J, Yeamans C, Hensley K, Friedman AD. C/EBPα:AP-1 leucine zipper heterodimers bind novel DNA element, activate the PU.1 promoter, and direct monocyte lineage commitment more potently than C/EBPα homodimers or AP-1. Oncogene 2008; 27: 2772–2779. https://doi.org/10.1038/sj.onc.1210940 PMID: 18026136
18. Heinz S, Benner C, Spann N, Bertolino E, Lin YC, Laslo P et al. Simple combinations of lineage-determining transcription factors prime cis-regulatory elements required for macrophage and B cell identities. Mol Cell. 2010; 38: 576–589. https://doi.org/10.1016/j.molcel.2010.05.004 PMID: 20513432
19. Liao X, Sharma N, Kapadia F, Zhou G, Lu Y, Hong H, et al. Krüppel-like factor 4 regulates macrophage polarization. J Clin Invest. 2011; 121: 2736–2749. https://doi.org/10.1172/JCI45444 PMID: 21670502
20. Ellwood-Yen K, Graeber TG, Wongvipat J, Iruela-Arispe ML, Zhang J, Matusik R, et al. Myc-driven murine prostate cancer shares molecular features with human prostate tumors. Cancer Cell 2003; 4: 223–238. PMID: 14522256

21. Tomayko MM, Reynolds CP. Determination of subcutaneous tumor size in athymic (nude) mice. Cancer Chemother Pharmacol. 1989; 24: 148–154. PMID: 2544306

22. Simons BW, Durham NM, Bruno TC, Grosso JF, Schaeffer AJ, Ross AE, et al. A human prostatic bacterial isolate alters the prostatic microenvironment and accelerates prostate cancer progression. J Pathol. 2015; 235: 478–489. https://doi.org/10.1002/path.4472 PMID: 25348195

23. Hume DA. Applications of myeloid-specific promoters in transgenic mice support in vivo imaging and functional genomics but do not support the concept of distinct macrophage and dendritic cell lineages or roles in immunity. J Leuk Biol. 2011; 89: 525–538.

24. Langley SR, Willeit K, Didangelos A, Matic LP, Skroblin P, Barallobre-Barreiro J, et al. Extracellular matrix proteomics identifies molecular signature of symptomatic carotid plaques. J Clin Invest. 2017; 127: 1546–1560. https://doi.org/10.1172/JCI86924 PMID: 28319050

25. Abram CL, Roberge GL, Hu Y, Lowell CA. Comparative analysis of the efficiency and specificity of myeloid-Cre deleting strains using ROSA-EYFP reporter mice. J. Immunol. Methods 2014; 408: 89–100. https://doi.org/10.1016/j.jim.2014.05.009 PMID: 24857755

26. Galkina E, Ley K. Immune and inflammatory mechanisms of atherosclerosis. Annu Rev Immunol. 2009; 27: 165–197. https://doi.org/10.1146/annurev.immunol.021908.132620 PMID: 19302038

27. Galkina E, Kadl A, Sanders J, Varughese D, Sarembock IJ, Ley K. Lymphocyte recruitment into the aortic wall before and during development of atherosclerosis is partially L-selectin dependent. J Exp Med. 2006; 203: 1273–1282. https://doi.org/10.1084/jem.20052205 PMID: 16682495

28. Sharma N, Lu Y, Zhou G, Liao X, Kapil P, Anand P, et al. Myeloid Krüppel-like factor 4 deficiency augments atherogenesis in ApoE-/- mice—brief report. Arterioscler Thromb Vasc Biol. 2012; 32: 2836–2838. https://doi.org/10.1161/ATVBAHA.112.300471 PMID: 23065827

29. Hamik A, Lin Z, Kumar A, Balcells M, Sinha S, Katz J, et al. Kruppel-like factor 4 regulates endothelial inflammation. J. Biol. Chem. 2007; 282: 13769–13779. https://doi.org/10.1074/jbc.M700078200 PMID: 17339326

30. Zhou G, Hamik A, Nayak L, Tian H, Shi H, Lu Y, et al. Endothelial Kruppel-like factor 4 protects against atherothrombosis in mice. J Clin Invest. 2012; 122: 4727–4731. https://doi.org/10.1172/JCI66056 PMID: 23160196

31. Comperat E, Egevad L, Camparo P, Roupret M, Vaessen C, Valdman A, et al. Clinical significance of intratumoral CD8+ regulatory T cells in prostate carcinoma. Anal Quant Cytol Histol. 2012; 32: 39–44.

32. Tang S, Moore ML, Grayson JM, Dubey P. Increased CD8+ T-cell function following castration and immunization is countered by parallel expansion of regulatory T cells. Cancer Res. 2012; 72: 1975–1985. https://doi.org/10.1158/0008-5472.CAN-11-2499 PMID: 22374980

33. Andreasen SØ, Thomsen AR, Koteliansky VE, Novobrantseva TI, Sprague AG, de Fougerolles AR, et al. Expression and functional importance of collagen-binding integrins, alpha 1 beta 1 and alpha 2 beta 1, on virus-activated T cells. J Immunol. 2003; 171: 2804–2811. PMID: 12960301

34. Ray SJ, Franki SN, Pierce RH, Dimitrova S, Koteliansky V, Sprague AG, Doherty PC, et al. The collagen binding alpha1beta1 integrin VLA-1 regulates CD8 T cell-mediated immune protection against heterologous influenza infection. Immunity 2004; 20: 167–179. PMID: 14975239

35. Richter M, Ray SJ, Chapman TJ, Austin SJ, Rebhahn J, Mosmann TR, et al. Collagen distribution and expression of collagen-binding α1β1 (VLA-1) and α2β1 (VLA-2) integrins on CD4 and CD8 T cells during influenza infection. J Immunol. 2007; 178: 4506–4516. PMID: 17372009

36. Overstreet MG, Gaylo A, Angermann BR, Hughson A, Hyun YM, Lambert K, et al. Inflammation-induced interstitial migration of effector $CD4^+$ T cells is dependent on integrin αV. Nat Immunol. 2013; 14: 949–958. https://doi.org/10.1038/ni.2682 PMID: 23933892

37. Shekhonin BV, Domogatsky SP, Idelson GL, Koteliansky VE, Rukosuev VS. Relative distribution of fibronectin and type I, III, IV, V collagens in normal and atherosclerotic intima of human arteries. Atherosclerosis 1987; 67: 9–16. PMID: 3314885

38. Hansson GK, Holm J, Jonasson L. Detection of activated T lymphocytes in the human atherosclerotic plaque. Am J Pathol. 1989; 135: 169–175. PMID: 2505620

39. Gewaltig J, Kummer M, Koella C, Cathomas G, Biedermann BC. Requirements for CD8 T-cell migration into the human arterial wall. Hum Pathol. 2008; 39: 1756–1762. https://doi.org/10.1016/j.humpath.2008.04.018 PMID: 18706675

40. Mrass P, Takano H, Ng LG, et al. Random migration precedes stable target cell interactions of tumor-infiltrating T cells. J Exp Med. 2006; 203: 2749–2761. https://doi.org/10.1084/jem.20060710 PMID: 17116735

41. Salmon H, Franciszkiewicz K, Damotte D, Dieu-Nosjean MC, Validire P, Trautmann A, et al. Matrix architecture defines the preferential localization and migration of T cells into the stroma of human lung tumors. J Clin Invest. 2012; 122: 899–910. https://doi.org/10.1172/JCI45817 PMID: 22293174

42. Knipper JA, Willenborg S, Brinckmann J, Bloch W, Maaß T, Wagener R, et al. Interleukin-4 receptor α rignaling in myeloid cells controls collagen fibril assembly in skin repair. Immunity 2015; 43: 803–816. https://doi.org/10.1016/j.immuni.2015.09.005 PMID: 26474656

*Presented as a poster at the Johns Hopkins University School of Medicine Sidney Kimmel Comprehensive Cancer Center 2018 Fellow Research Day (June 14, 2018)*

Authors: Suresh, Rahul; Barakat, David J.; Gilmore, Gary L.; Simons, Brian W.; Pienta, Kenneth J. and Friedman, Alan D.
(Department of Oncology/Division of Pediatric Oncology)

Title: ADOPTIVE TRANSFER OF NF-KB P50 DEFICIENT MYELOID CELLS AS A COMPONENT OF PROSTATE CANCER IMMUNOTHERAPY

Abstract: **Background:** Prostate carcinoma is the most common male malignancy. Despite extending survival, androgen depravation therapy invariably leads to the development of lethal castration resistant prostate cancer. Myeloid cells are a major component of the prostate cancer microenvironment. Peripheral blood monocytes are recruited to the tumor where they undergo differentiation into tumor-associated macrophages and dendritic cells. Tumor cells further secrete cytokines that activate a genetic program, including increased nuclear expression of the inhibitory NF-kB p50 subunit, to suppress myeloid cell pro-inflammatory functions and prevent subsequent immune response. Promoting macrophage and dendritic cell activation represents an attractive component of immunotherapy.

**Methods:** Wild-type or NF-kB p50-/- B6 mice were inoculated subcutaneously with a syngeneic Hi-Myc prostate tumor line, followed by evaluation of tumor growth and tumor myeloid and T cell phenotypes. For monocyte adoptive transfer, marrow from WT and p50-/- mice was subject to lineage-depletion followed by culture in IMDM with FBS and TPO/SCF/FLT3L (cytokines expected to maintain myeloid progenitor immaturity) for 6d followed by 1-2d culture in GM-CSF or M-CSF. These formed immature monocytes and DCs, with those in M-CSF appearing less activated. 5-FU was given when tumors forming in WT hosts were small (to reduce marrow competition and endogenous TAMs), followed by tail vein infusion of 10E6 expanded WT or p50-/- monocytes x 3 doses, or PBS as control.

**Results:** Prostate tumors grew slower in p50-/- mice compared to WT recipients, with increased tumor myeloid and T cell numbers and activation. *Ex vivo* expanded p50-/- immature myeloid cells (IMC) localized to tumors and draining lymph nodes to form activated myeloid cells. They also restricted prostate tumor growth in comparison to WT monocytes or 5-FU alone. Responses were also seen syngeneic GBM and pancreatic ductal carcinoma models. In addition, infusion of p50-IMC enhanced prostate tumor and draining lymph node T cell infiltration and activation.

**Conclusions:** Many solid tumors are refractory to checkpoint blockade, which may in part reflect suppression of T cell activation or priming by tumor or nodal myeloid cells. We find that infusion of immature myeloid cells lacking NF-kB p50, with capacity to generate activated TAMs and DCs, slows the growth of subcutaneously injected prostate tumors, associated with T cell recruitment and activation. NF-kB p50 CRISPR/Cas9 genomic deletion or shRNA knockdown during *ex vivo* expansion of patient bone marrow or peripheral blood myeloid progenitors may enable infused myeloid cells to obtain a pro-inflammatory phenotype that could synergize with T cell activating tumor vaccines or checkpoint inhibitors in prostate cancer and additional solid tumors.

# NF-κB p50 DEFICIENT IMMATURE MYELOID CELLS AND THEIR USE IN TREATMENT OF CANCER

## STATEMENT OF GOVERNMENTAL INTEREST

**[0001]** This invention was made with government support under grant no. W81XWH-16-1-0334 awarded by the Department of Defense. The government has certain rights in the invention.

## BACKGROUND OF THE INVENTION

**[0002]** In the U.S. population, mortality associated with the 15 most common cancer types alone has been estimated to approach 170 deaths annually per 100,000 individuals. Currently, there are an estimated 1,437,180 new cases of cancer and 565,650 deaths each year. The economic burden of cancer has been estimated to exceed $96B in 1990 dollars.

**[0003]** The nuclear factor kappa-light-chain-enhancer of activated B cells (NF-κB) activates inflammatory pathways in myeloid cells in response to extra-cellular signals. The canonical NF-κB subunits are p65 and p50; both contain the Rel Homology Domain that mediates homo- or hetero-dimerization and DNA-binding, with p65 also having a trans-activation domain. NF-κB p50 (p50) is an inhibitory subunit; in the basal state p65 is held in the cytoplasm by IκB, whereas p50:p50 homo-dimers enter the nucleus, bind DNA, and repress gene expression. Absence of p50 leads to activation of pro-inflammatory pathways.[1-3]

**[0004]** T cell checkpoint inhibition has emerged as a novel cancer therapeutic approach effective in a subset of cancer patients. Effectiveness of T cell checkpoint inhibition is often limited by T cell-suppressive tumor myeloid cells. Thus, there exists an urgent need to improve cancer immunotherapy. Development of novel approaches that augment T cell checkpoint therapy, or that augment other treatments designed to increase anti-tumor T cell immunity such as tumor vaccines, will lead to clinical benefit for a large number of cancer patients.

**[0005]** Clinical trials have been conducted in cancer patients using mature macrophages, typically generated from blood monocytes using GM-CSF, activated using IFNγ, and provided intravenously (IV); these trials were largely unsuccessful, with the exception of instillation of macrophages into the bladder of patients with bladder cancer, which proved

less effective than standard therapy.[4,5] When radio-labeled and provided to patients IV, macrophages were seen in lung, liver, and spleen, but not tumors, perhaps limiting their efficacy,[4] inspiring the present inventor to consider infusion of immature myeloid cells (IMC) that might more effectively reach tumors.

**[0006]** Infusion of anti-inflammatory, M2-polarized macrophages into mice with autoimmune encephalitis reverses CNS lesions, and infusion of murine bone marrow-derived monocytes similarly polarized to an immunosuppressive state reduces graft versus host disease (GVHD).[6,7] Infused monocytes are more effective against GVHD if they are genetically modified, by deletion of both copies of the ASC gene, to retain their anti-inflammatory state *in vivo*,[7] inspiring the present inventor to consider the utility of infusing pro-inflammatory IMC having absent or reduced NF-κB p50 as therapy for cancer.

## SUMMARY OF THE INVENTION

**[0007]** The present inventor has now developed methods for expanding myeloid progenitors from p50-/- or WT mice and find that adoptive cell transfer (ACT) of p50-/- immature myeloid cells, given after a single dose of 5-fluorouracil (5FU), leads to tumor responses in three cancer models, glioblastoma, prostate carcinoma, and pancreatic ductal carcinoma.

**[0008]** In accordance with one or more embodiments, the present invention provides methods for making autologous bone marrow hematopoietic progenitors wherein the NF-κB p50 protein subunit of said progenitor cell or cells is absent or reduced.

**[0009]** The progenitor cells are expanded, exposed to a myeloid cytokine or cytokines, and can be used to treat various malignancies. The infused cells, designated p50-immature myeloid cells (p50-IMC), have the potential to generate mature granulocytes, monocytes, macrophages, and dendritic cells in vivo that are activated due to the absence of p50. Methods for the genetically manipulation of a subject's hematopoietic progenitors during the expansion phase to reduce or eliminate p50 expression are also contemplated, and the use of the inventive progenitor cells may be combined with chemotherapy or other therapeutic agents to maximize efficacy.

**[0010]** In some embodiments, the therapeutic agents that might augment p50-IMC anti-cancer efficacy include but are not limited to radiation therapy, T cell checkpoint inhibitors,

epigenetic modulators, CSF1R antibodies or chemical inhibitors, metabolic modulators, tumor or dendritic cell vaccines, and myeloid cytokines.

**[0011]** In accordance with an embodiment, the present invention provides a synthetic hematopoietic progenitor cell or population of cells, wherein the NF-κB p50 protein subunit of said cell or cells is absent or reduced.

**[0012]** In accordance with an embodiment, the present invention provides a pharmaceutical composition comprising a synthetic hematopoietic progenitor cell or population of cells, wherein the NF-κB p50 protein subunit of said cell or cells is absent or reduced, and a pharmaceutically acceptable carrier.

**[0013]** In accordance with an embodiment, the present invention provides a pharmaceutical composition comprising a synthetic hematopoietic progenitor cell or population of cells, wherein the NF-κB p50 protein subunit of said cell or cells is absent or reduced, a pharmaceutically acceptable carrier, and at least one or more additional biologically active agents.

**[0014]** In accordance with an embodiment, the present invention provides a method of treating cancer in a subject in need thereof, comprising administering to the subject a therapeutically effective amount of said cells or said pharmaceutical compositions described herein.

**[0015]** In accordance with an embodiment, the present invention provides a method for making a synthetic hematopoietic progenitor cell or population of cells, wherein the NF-κB p50 protein subunit of said cell or cells is absent or reduced, comprising obtaining bone marrow or blood cells from a mammal, isolating a population that includes hematopoietic stem and progenitor cells (e.g. isolation of lineage-negative or CD34+ cells), expanding these cells in vitro in the presence of FL, TPO, and SCF, and potentially additional or alternative cytokine combinations or other biologically activate agents that maintain cell immaturity, while introducing reagents designed to knockout (KO) their p50 genes or knockdown (KD) their p50 mRNAs encoding p50 protein, and to then culture the cells with M-CSF and/or other myeloid cytokines that might include GM-CSF, IL-4, and FL to generate p50-IMC.

## BRIEF DESCRIPTION OF THE DRAWINGS

**[0016]** Figure 1A-1B illustrates an embodiment of a method for making a synthetic hematopoietic immature myeloid cell population, wherein the NF-κB p50 protein subunit of said cell or cells is absent or reduced. The bone marrow from a p50-/- knockout mouse is flushed from the extremity bones and subjected to red blood cell lysis using ammonium chloride. Lineage-negative cells are isolated using a magnetic column after staining with a cocktail of antibodies that bind mature blood cells. These cells are then expanded for 6 days in IMDM media with heat-inactivated fetal bovine serum (HI-FBS) and the FL, TPO, and SCF cytokines, with penicillin/streptomycin (P/S). These cytokines maintain cell immaturity, leading to a blast-like morphology upon Wright-Giemsa staining, as shown for cells expanded from the marrow of a p50-/- mouse (1A, left). The cells are then transferred to IMDM with HI-FBS, P/S, and M-CSF for 1 day in ultra-low attachment plates, inducing an immature myeloid morphology in the majority of the cells (1A, right). At this point ~87% of the cells express than pan-myeloid CD11b surface marker upon flow cytometry (FC), with ~57% of CD11b+ cells expressing the monocyte and macrophage marker MCSFR and ~22% instead expressing the dendritic cell (DC) marker FLT3 and CD11c (1B). 6% of the cells express the Ly6G granulocyte marker and none express the CD3 T cell or CD19 B cell markers (not shown). Cells obtained using the same protocol using WT marrow have similar morphologic and FACS characteristics.

**[0017]** Figure 1C-1E evaluates the in vivo localization of IMC. Wild-type (WT)-IMC cells were generated from CMV-Luc mice harboring a luciferase transgene. When a single dose of WT-IMC cells was infused into PDC, glioma, or PCa tumor-bearing mice, 5 days after a dose of 5-fluorouracil (5FU), a subset of cells reach the tumor, with some cells also localizing to lung, spleen, and bone marrow (1C). Additional experiments utilize the CD45.1/CD45.2 congenic allele pair. CD45.1 B6 mice implanted with pancreatic ductal carcinoma (PDC) received 5FU followed by two infusions of 1E7 CD45.2+ p50-IMC on day 12 (d12) and d14. Analysis on d16 shows that 8% of CD11b+ tumor myeloid cells derived from p50-IMC (1D). WT CD45.1 mice inoculated with prostate carcinoma (PCa) cells received 5FU on d13 followed by a single dose of CD45.2+ p50-IMC on d18. 2% of tumor on d2, and 13% of bone marrow (BM), 24% of spleen, and 1.4% of inguinal node CD11b+ myeloid cells on d6 derived from CD45.2+ p50-IMC (1E).

**[0018]** Figure 1F evaluates the nature of myeloid cells derived from p50-IMC in vivo. The majority of PCa tumor $CD45.2^{+}CD11b^{+}$ cells express F4/80, CD11c, and MHCII, indicative of activated macrophages and/or DCs, whereas few tumor CD45.2+CD11b+ cells express the granulocytic Ly6G marker (1F, top), and a similar pattern is seen within the tumor-draining inguinal nodes (not shown). In contrast, p50-IMC-derived marrow cells express variable F4/80 and little CD11c or the MHCII activation marker, with a prominent Ly6G+ subset, indicative of donor-derived macrophages and granulocytes (1F, bottom), and a similar pattern was evident in spleen (not shown). Thus, p50-IMC form activated tumor and lymph node myeloid cells, with marrow and spleen potentially providing an ongoing reservoir.

**[0019]** Figure 2 evaluates the effects of p50-IMC on tumor T cells. WT CD45.1+ mice inoculated with Hi-Myc PCa cells received 5FU on day 13 followed by 1 x $10^7$ CD45.2+ WT-IMC (n=5) or p50-IMC (n=4) on days 18, 21, and 25. Six days later, tumor cells were analyzed for CD3+CD4+ and CD3+CD8+ T cells within the CD45.2+ gate (2A), showing that p50-IMC increase tumor CD8 T cell ~5-fold. Tumor CD4 and CD8 T cells were analyzed for intracellular IFNγ, 4 hours after exposure to vehicle or PMA/ionomycin, with brefeldin A/monensin protein transport inhibitors, showing that p50-IMC increase IFNγ+ activated tumor T cells ~2-fold (2B). Tumor CD8 T cells were analyzed for PD-1 (2C), showing ~2-fold increased T cell PD-1 after p50-IMC, supporting the potential utility of combining p50-IMC with anti-PD-1 T cell checkpoint inhibitors.

**[0020]** Figure 3 demonstrates anti-cancer efficacy of p50-IMC. Ten mice inoculated SQ with Hi-Myc B6 prostate cancer cells[8,9] showed significantly slower tumor growth after receiving 5FU (150 mg/kg) on day 13 followed by 1 x $10^7$ p50-IMC on days 18, 21, and 25, compared to 10 mice receiving WT myeloid cells or 5 mice receiving 5-fluorouracil (5FU) alone (3A). Mice implanted in the brain with GL261-Luc glioblastoma (GBM) cells[10,11] received 5FU on day 3, followed by no myeloid cells, p50-IMC or WT-IMC on days 8, 11, and 14, and In Vivo Imaging System (IVIS) imaging on d21 (3B). While the 5FU or 5FU+WT-IMC groups had mice with large tumors or mice that died of tumors (indicated by XX), 3 of 5 mice subjected to p50-IMC ACT developed very small GBM tumors, with one having a large tumor and one having died prior to d21 (X). Finally, 4 of 10 mice inoculated in the pancreas with PDC-Luc cells showed marked regression in tumor size in response to 5FU+p50-IMC, but not 5FU+WT-IMC or 5FU alone (3C) – data in the left panel were obtained by providing 5FU on day 7, followed by p50-IMC on days 12, 15, and 19; data in

the right panel were obtained by providing 5FU on day 3, following by WT-IMC or p50-IMC cells on days 7, 10, and 12 (note that tumor size is on a log scale). PDC-Luc cells were generated by introducing the Luc2 luciferase cDNA was into the UN-KC-6141 line.[12] 5FU is given to reduce marrow competition with infused IMC and to reduce tumor myeloid cell numbers.[13]

**[0021]** Figure 4 demonstrates CRISPR/Cas9 knockout (KO) of the p50 gene in murine or human myeloid cell lines and shRNA knockdown (KD) of p50 mRNA in murine marrow myeloid progenitors, illustrative of alternative approaches that can be taken to develop human p50-IMC from patient hematopoietic cells for clinical application wherein the NF-κB p50 protein subunit of said cell or cells is absent or reduced. M1 murine or U937 human myeloid cell lines were transduced with lentiCRISPRv2 plasmids encoding either a non-targeting sgRNA (NTV), mouse or human p50 gene-directed sgRNAs, hSpCas9, and puromycin-resistance. After selection in puromycin for 7d, pooled M1 or U937 cells were subjected to Western blotting for p50 and β-actin. Relative expression of p50 protein, normalized to β-actin, is shown below each lane (4A). PCR amplification of a fragment surrounding the Cas9 cut site of targeted and control cells followed by DNA sequencing and analysis with TIDE software evaluates p50 alleles;[14] TIDE analysis of M1 lines sg2, sg3, and sg5 shows 78-93% allele targeting (not shown), with U937 sg1 cells having 89% p50 gene KO (4B). Murine BM, isolated 5d after 5FU, were cultured in IMDM/FBS with SCF/FL/TPO and transduced with pLKO.1 lentiviral vectors expressing a non-targeting shRNA (NTV) or p50-directed shRNAs. After puromycin selection and transfer to M-CSF for 1d, total cellular proteins were evaluated for p50 and β-actin (4C).

## DETAILED DESCRIPTION OF THE INVENTION

**[0022]** In accordance with an embodiment, the present invention provides a synthetic hematopoietic progenitor cell or population of cells, wherein the NF-κB p50 protein subunit of said cell or cells is absent or reduced.

**[0023]** In some embodiments, the present invention provides compositions, methods, and systems for generating synthetic hematopoietic progenitor cell or population of cells, wherein the NF-κB p50 protein subunit of said cell or cells is absent or reduced.

**[0024]** In some embodiments, the present invention provides compositions, systems, and methods for administering synthetic hematopoietic progenitor cell or population of cells, wherein the NF-κB p50 protein subunit of said cell or cells is absent or reduced to a subject (e.g., to a subject with cancer in an adoptive transfer type of procedure).

**[0025]** In some embodiments, these cells where NF-κB p50 protein subunit of said cell or cells is absent or reduced are termed immature myeloid cells (IMC) or "p50-IMC".

**[0026]** In some embodiments, p50-IMC are generated from mammals such as mice lacking both copies of the gene encoding p50. In some alternative embodiments, p50-IMC are generated from hematopoietic cells, such as those obtained from a cancer patient, using gene editing tools such as CRISPR/Cas9 to knockout (KO) one or both p50 gene alleles in a subset of the cells. In some embodiments, p50-IMC are generated from hematopoietic cells, such as those obtained from a cancer patient, using agents that knockdown (KD) expression of p50 mRNA, such as shRNA, siRNA, anti-sense DNA, or anti-sense RNA. In some embodiments, p50-IMC express the monocyte markers CD11b, MCSFR, CD14, CD64, and/or CD16. In some embodiments, IMC express the dendritic cell markers HLA-DR, CD209, and/or FLT3. In other embodiments, IMC can also express CD11c, CD1c, CD141, CD303, CD304, CD1a, CD15, CD13, and/or CD33.

**[0027]** In accordance with an embodiment, the present invention provides a pharmaceutical composition comprising a synthetic hematopoietic progenitor cell or population of cells, wherein the NF-κB p50 protein subunit of said cell or cells is absent or reduced, and a pharmaceutically acceptable carrier.

**[0028]** In accordance with an embodiment, the present invention provides a pharmaceutical composition comprising a synthetic hematopoietic progenitor cell or population of cells, wherein the NF-κB p50 protein subunit of said cell or cells is absent or reduced, a pharmaceutically acceptable carrier, and at least one or more additional biologically active agents.

**[0029]** In accordance with an embodiment, the present invention provides a method of treating cancer in a subject in need thereof, comprising administering to the subject a therapeutically effective amount of said cells or said pharmaceutical compositions described herein.

**[0030]** As used herein, the term "wherein the NF-κB p50 protein subunit of said cell or cells is absent or reduced" means that the p50 protein subunit is not expressed in the cell or population of cells at detectable levels, or the level of expression of the p50 protein subunit in

the cell or population of cells is less than the level of expression of a control or a wild-type cell or population of cells.

**[0031]** As used herein, the term "regression" refers to the return of a diseased subject, cell, tissue, or organ to a non-pathological, or less pathological state as compared to basal nonpathogenic exemplary subject, cell, tissue, or organ. For example, regression of a tumor includes a reduction of tumor mass as well as complete disappearance of a tumor or tumors.

**[0032]** As used herein the term, "in vitro" refers to an artificial environment and to processes or reactions that occur within an artificial environment. In vitro environments can consist of, but are not limited to, test tubes and cell cultures. The term "in vivo" refers to the natural environment (e.g., an animal or a cell) and to processes or reactions that occur within a natural environment.

**[0033]** As used herein, the term "cell culture" refers to any in vitro culture of cells. Included within this term are continuous cell lines (e.g., with an immortal phenotype), primary cell cultures, finite cell lines (e.g., non-transformed cells), and any other cell population maintained in vitro.

**[0034]** In some embodiments, the p50-IMC can be further expanded in vitro by exposure to IL-3, IL-6, Notch ligands or aryl hydrocarbon antagonists.[15,16]

**[0035]** In some embodiments, the inventive methods include when a patient receives immunotherapy with one or more checkpoint inhibitors, prior to, at the same time, and/or after receiving the p50-IMC by adoptive transfer IV, or prior to, at the same time, and/or after direct administration of p50-IMC to the patient's tumor. In various embodiments, the checkpoint inhibitor(s) target one or more of CTLA-4 or PD-1/PD-L1, and/or other checkpoint inhibitors such as LAG-3 or TIM-3, which may include antibodies against such targets, such as monoclonal antibodies, or portions thereof, or humanized or fully human versions thereof. In some embodiments, the checkpoint inhibitor therapy comprises Yervoy (ipilimumab) or Keytruda (pembrolizumab).

**[0036]** In some embodiments, the inventive methods include when the patient receives a tumor or dendritic cell vaccine prior to, at the same time, and/or after receiving the p50-IMC by adoptive transfer IV, or prior to, at the same time, and/or after direct administration of p50-IMC to the patient's tumor. In various embodiments, the tumor vaccine might be autologous tumor cells expressing GM-CSF or tumor cells mixed with other cells expressing GM-CSF. In some embodiments, the dendritic cell vaccine may be patient dendritic cells primed with a tumor antigen.

**[0037]** In some embodiments, the inventive methods include when the patient receives radiation therapy to the tumor prior to or subsequent to receiving p50-IMC by adoptive transfer IV or prior to or subsequent to direct administration of p50-IMC to the patient's tumor.

**[0038]** In some embodiments, the inventive methods include when the patient receives about 1 to 5 rounds of adoptive immunotherapy (e.g., one, two, three, four or five rounds) with the p50-IMC. In some embodiments, each administration of adoptive immunotherapy is conducted prior to (e.g., from about 1 day to about 1 week prior to), simultaneously with, or after (e.g., from about 1 day to about 1 week after), a round of checkpoint inhibitor therapy.

**[0039]** In particular embodiments, the inventive methods further comprise administering the synthetic hematopoietic progenitor cell or population of cells, the p50-IMC to a subject (e.g. a patient). In some embodiments, the subject has a tumor and the contacting reduces the size (or eliminates) the tumor.

**[0040]** The subject referred to in the inventive methods can be any host. Preferably, the host is a mammal. As used herein, the term "mammal" refers to any mammal, including, but not limited to, mammals of the order Rodentia, such as mice and hamsters, and mammals of the order Lagomorpha, such as rabbits. It is preferred that the mammals are from the order Carnivora, including Felines (cats) and Canines (dogs). It is more preferred that the mammals are from the order Artiodactyla, including Bovine (cows) and Swine (pigs) or of the order Perssodactyla, including Equine (horses). It is most preferred that the mammals are of the order Primates, Ceboids, or Simoids (monkeys) or of the order Anthropoids (humans and apes). An especially preferred mammal is the human.

**[0041]** In some embodiments, the inventive methods further comprise administering to the subject cytokines active on myeloid or T cells that might include M-CSF, G-CSF, GM-CSF, FL, IL-4, IL-2, and/or IL-15, or chemical mimetics mimicking the action of one or more of these cytokines. In certain embodiments, after a subject has been treated with the adoptive transfer methods and compositions of the present invention, diagnostic procedures are employed to determine efficacy. In certain embodiments, tumor regression is analyzed. For example, clinical and radiographic responses (e.g. MRI and CT) can be used for monitoring the effector tumor-reactive p50-IMC on tumor growth. Certain procedures include clinical, histological and bioluminescent in vivo imaging for monitoring tumor growth. In some embodiments, the persistence of functional p50-IMC is monitored by isolation of myeloid cells from tumor or draining lymph node followed by analysis for p50 mRNA or protein

expression or p50 gene deletion or by staining tumor or lymph node tissue for proteins or RNAs expressed in activated myeloid cells, including in macrophages and dendritic cells. In other embodiments, the ability of p50-IMC to induce an anti-tumor T cell response is monitored by staining tumor or lymph node tissue for total and activated CD4 and CD8 T cells and for regulatory T cells or by isolation of tumor or lymph node T cell followed FC or RNA isolation and mRNA analysis.

**[0042]** Administration and Dosing Regimes.

**[0043]** One skilled in the art will appreciate that administration and dosing of cells for adoptive transfer may need to be customized to the patient for highest efficacy and tolerance. In human patients, this translates to a dose of about $3\times10^8$ p50-IMC cells, although higher and lower amounts of cells (e.g. one or more orders of magnitude different) may be employed. It is noted that, in certain embodiments, the number of p50-IMC cells that is needed for therapeutic treatment using the methods and compositions of the present invention is generally less than disclosed in the prior art. For example, in some embodiments, the amount of the p50-IMC applied to the patient can be e.g., $3\times10^7$ to $1\times10^8$ cells. It is further noted that while repeated transplantation can improve the efficacy of p50-IMC -mediated anti-tumor activity, embodiments of the present invention may employ one or more administrations of the p50-IMC. Such therapy may be sufficient for therapeutic treatment and may be further augmented by repeated checkpoint inhibitor, tumor or dendritic cell vaccine, and cytokine therapy.

**[0044]** Types of Cancer.

**[0045]** Methods of some embodiments of the present invention find use in the treatment of cancer and are not limited by the type of cancer. In some embodiments, methods may be directed towards treatment of solid tumors. Examples of solid tumors include sarcomas and carcinomas such as, but not limited to: fibrosarcoma, myxosarcoma, liposarcoma, chondrosarcoma, osteogenic sarcoma, chordoma, angiosarcoma, endotheliosarcoma, lymphangiosarcoma, lymphangioendotheliosarcoma, synovioma, mesothelioma, Ewing's tumor, leiomyosarcoma, rhabdomyosarcoma, colon carcinoma, pancreatic cancer, breast cancer, ovarian cancer, prostate cancer, squamous cell carcinoma, basal cell carcinoma, adenocarcinoma, sweat gland carcinoma, sebaceous gland carcinoma, papillary carcinoma, papillary adenocarcinomas, cystadenocarcinoma, medullary carcinoma, bronchogenic carcinoma, renal cell carcinoma, hepatoma, bile duct carcinoma, choriocarcinoma, seminoma, embryonal carcinoma, Wilms' tumor, cervical cancer, testicular tumor, lung

carcinoma, small cell lung carcinoma, bladder carcinoma, epithelial carcinoma, glioma, astrocytoma, medulloblastoma, craniopharyngioma, ependymoma, pinealoma, hemangioblastoma, acoustic neuroma, oligodendroglioma, meningioma, melanoma, neuroblastoma, and retinoblastoma. Additional types of malignancies and related disorders include but are not limited to leukemia (acute leukemia, acute lymphocytic leukemia, acute myelocytic leukemia, myeloblastic, promyelocytic, myelomonocytic, monocytic, erythroleukemia, chronic leukemia, chronic myelocytic (granulocytic) leukemia, chronic lymphocytic leukemia), polycythemia vera, lymphoma (Hodgkin's disease, non-Hodgkin's disease), multiple myeloma, Waldenström's macroglobulinemia, melanoma, sarcoma, and heavy chain disease.

**[0046]** It will be understood by those of ordinary skill in the art that the term "tumor" as used herein means a neoplastic growth which may, or may not be malignant. Additionally, the compositions and methods provided herein are not only useful in the treatment of tumors, but in their micrometastses and their macrometastses. Typically, micrometastasis is a form of metastasis (the spread of a cancer from its original location to other sites in the body) in which the newly formed tumors are identified only by histologic examination; micrometastases are detectable by neither physical exam nor imaging techniques. In contrast, macrometastses are usually large secondary tumors.

**[0047]** Co-administration with chemotherapeutic agents.

**[0048]** Chemotherapy and the adoptive p50-IMC cell transfer of the present invention may be performed sequentially or simultaneously. For example, myeloid depleting chemotherapy may be conducted prior to adoptive cell transfer. The present invention is not limited by type of anti-cancer agent co-administered. Indeed, a variety of anti-cancer agents are contemplated to be useful in the present invention including, but not limited to, Acivicin; Aclarubicin; Acodazole Hydrochloride; Acronine; Adozelesin; Adriamycin; Aldesleukin; Alitretinoin; Allopurinol Sodium; Altretamine; Ambomycin; Ametantrone Acetate; Aminoglutethimide; Amsacrine; Anastrozole; Annonaceous Acetogenins; Anthramycin; Asimicin; Asparaginase; Asperlin; Azacitidine; Azetepa; Azotomycin; Batimastat; Benzodepa; Bexarotene; Bicalutamide; Bisantrene Hydrochloride; Bisnafide Dimesylate; Bizelesin; Bleomycin Sulfate; Brequinar Sodium; Bropirimine; Bullatacin; Busulfan; Cabergoline; Cactinomycin; Calusterone; Caracemide; Carbetimer; Carboplatin; Carmustine; Carubicin Hydrochloride; Carzelesin; Cedefingol; Celecoxib; Chlorambucil; Cirolemycin; Cisplatin; Cladribine; Crisnatol Mesylate; Cyclophosphamide; Cytarabine; Dacarbazine;

DACA (N-[2-(Dimethyl-amino)ethyl]acridine-4-carboxamide); Dactinomycin; Daunorubicin Hydrochloride; Daunomycin; Decitabine; Denileukin Diftitox; Dexormaplatin; Dezaguanine; Dezaguanine Mesylate; Diaziquone; Docetaxel; Doxorubicin; Doxorubicin Hydrochloride; Droloxifene; Droloxifene Citrate; Dromostanolone Propionate; Duazomycin; Edatrexate; Eflornithine Hydrochloride; Elsamitrucin; Enloplatin; Enpromate; Epipropidine; Epirubicin Hydrochloride; Erbulozole; Esorubicin Hydrochloride; Estramustine; Estramustine Phosphate Sodium; Etanidazole; Ethiodized Oil I 131; Etoposide; Etoposide Phosphate; Etoprine; Fadrozole Hydrochloride; Fazarabine; Fenretinide; Floxuridine; Fludarabine Phosphate; Fluorouracil; 5-FdUMP; Fluorocitabine; Fosquidone; Fostriecin Sodium; FK-317; FK-973; FR-66979; FR-900482; Gemcitabine; Geimcitabine Hydrochloride; Gemtuzumab Ozogamicin; Gold Au 198; Goserelin Acetate; Guanacone; Hydroxyurea; Idarubicin Hydrochloride; Ifosfamide; Ilmofosine; Interferon Alfa-2a; Interferon Alfa-2b; Interferon Alfa-n1; Interferon Alfa-n3; Interferon Beta-1a; Interferon Gamma-1b; Iproplatin; Irinotecan Hydrochloride; Lanreotide Acetate; Letrozole; Leuprolide Acetate; Liarozole Hydrochloride; Lometrexol Sodium; Lomustine; Losoxantrone Hydrochloride; Masoprocol; Maytansine; Mechlorethamine Hydrochloride; Megestrol Acetate; Melengestrol Acetate; Melphalan; Menogaril; Mercaptopurine; Methotrexate; Methotrexate Sodium; Methoxsalen; Metoprine; Meturedepa; Mitindomide; Mitocarcin; Mitocromin; Mitogillin; Mitomalcin; Mitomycin; Mytomycin C; Mitosper; Mitotane; Mitoxantrone Hydrochloride; Mycophenolic Acid; Nocodazole; Nogalamycin; Oprelvekin; Ormaplatin; Oxisuran; Paclitaxel; Pamidronate Disodium; Pegaspargase; Peliomycin; Pentamustine; Peplomycin Sulfate; Perfosfamide; Pipobroman; Piposulfan; Piroxantrone Hydrochloride; Plicamycin; Plomestane; Porfimer Sodium; Porfiromycin; Prednimustine; Procarbazine Hydrochloride; Puromycin; Puromycin Hydrochloride; Pyrazofurin; Riboprine; Rituximab; Rogletimide; Rolliniastatin; Safingol; Safingol Hydrochloride; Samarium/Lexidronam; Semustine; Simtrazene; Sparfosate Sodium; Sparsomycin; Spirogermanium Hydrochloride; Spiromustine; Spiroplatin; Squamocin; Squamotacin; Streptonigrin; Streptozocin; Strontium Chloride Sr 89; Sulofenur; Talisomycin; Taxane; Taxoid; Tecogalan Sodium; Tegafur; Teloxantrone Hydrochloride; Temoporfin; Teniposide; Teroxirone; Testolactone; Thiamiprine; Thioguanine; Thiotepa; Thymitaq; Tiazofurin; Tirapazamine; Tomudex; TOP-53; Topotecan Hydrochloride; Toremifene Citrate; Trastuzumab; Trestolone Acetate; Triciribine Phosphate; Trimetrexate; Trimetrexate Glucuronate; Triptorelin; Tubulozole Hydrochloride; Uracil Mustard; Uredepa; Valrubicin; Vapreotide; Verteporfin; Vinblastine; Vinblastine Sulfate; Vincristine; Vincristine Sulfate;

Vindesine; Vindesine Sulfate; Vinepidine Sulfate; Vinglycinate Sulfate; Vinleurosine Sulfate; Vinorelbine Tartrate; Vinrosidine Sulfate; Vinzolidine Sulfate; Vorozole; Zeniplatin; Zinostatin; Zorubicin Hydrochloride; 2-Chlorodeoxyadenosine; 2′-Deoxyformycin; 9-aminocamptothecin; raltitrexed; N-propargyl-5,8-dideazafolic acid; 2-chloro-2′-arabino-fluoro-2′-deoxyadenosine; 2-chloro-2′-deoxyadenosine; anisomycin; trichostatin A; hPRL-G129R; CEP-751; linomide; sulfur mustard; nitrogen mustard (mechlorethamine); cyclophosphamide; melphalan; chlorambucil; ifosfamide; busulfan; N-methyl-N-nitrosourea (MNU); N,N′-Bis(2-chloroethyl)-N-nitrosourea (BCNU); N-(2-chloroethyl)-N′-cyclohex-yl-N-nitrosourea (CCNU); N-(2-chloroethyl)-N′-(trans-4-methylcyclohexyl-N-nitrosourea (MeCCNU); N-(2-chloroethyl)-N′-(diethyl)ethylphosphonate-N-nit-rosourea (fotemustine); streptozotocin; diacarbazine (DTIC); mitozolomide; temozolomide; thiotepa; mitomycin C; AZQ; adozelesin; Cisplatin; Carboplatin; Ormaplatin; Oxaliplatin; C1-973; DWA 2114R; JM216; JM335; Bis (platinum); tomudex; azacitidine; cytarabine; gemcitabine; 6-Mercaptopurine; 6-Thioguanine; Hypoxanthine; teniposide; 9-amino camptothecin; Topotecan; CPT-11; Doxorubicin; Daunomycin; Epirubicin; darubicin; mitoxantrone; losoxantrone; Dactinomycin (Actinomycin D); amsacrine; pyrazoloacridine; all-trans retinol; 14-hydroxy-retro-retinol; all-trans retinoic acid; N-(4-Hydroxyphenyl) retinamide; 13-cis retinoic acid; 3-Methyl TTNEB; 9-cis retinoic acid; fludarabine (2-F-ara-AMP); and 2-chlorodeoxyadenosine (2-Cda).

**[0049]** With respect to the pharmaceutical compositions used in combination with the p50-IMC described herein, the carrier can be any of those conventionally used for cell therapy, and is limited only by considerations such as cell viability and by the route of administration. The carriers described herein are well-known to those skilled in the art and are readily available to the public. It is preferred that the carrier be one which is chemically inert to the active agent(s), and one which has little or no detrimental side effects or toxicity under the conditions of use. Examples of the carriers include tissue culture media or buffered saline, and these carriers may include cytokines used to generate p50-IMC.

**[0050]** The choice of carrier will be determined, in part, by the particular pharmaceutical composition, as well as by the particular method used to administer the composition. Accordingly, there are a variety of suitable formulations of the pharmaceutical composition of the invention.

**[0051]** It will be understood to those of skill in the art that the term “chemotherapeutic agent” is any agent capable of affecting the structure or function of the body of a subject or is

an agent useful for the treatment or modulation of a disease or condition in a subject suffering therefrom. Examples of therapeutic agents can include any drugs known in the art for treatment of disease indications, including, for example, cancer.

**[0052]** An active agent and a biologically active agent are used interchangeably herein to refer to a chemical or biological compound, including cells that induce a desired pharmacological and/or physiological effect, wherein the effect may be prophylactic or therapeutic.

**[0053]** The dose of the chemotherapeutic agents used in conjunction with the p50-IMC of the present invention also will be determined by the existence, nature and extent of any adverse side effects that might accompany the administration of a particular composition. Typically, an attending physician will decide the dosage of the pharmaceutical composition with which to treat each individual subject, taking into consideration a variety of factors, such as age, body weight, general health, diet, sex, compound to be administered, route of administration, and the severity of the condition being treated. By way of example, and not intending to limit the invention, the dose of one or more chemotherapeutic agents used in conjunction with p50-IMC can be about 0.001 to about 1000 mg/kg body weight of the subject being treated, from about 0.01 to about 100 mg/kg body weight, from about 0.1 mg/kg to about 10 mg/kg, and from about 0.5 mg to about 5 mg/kg body weight.

**[0054]** The dose of the compositions of the present invention also will be determined by the existence, nature and extent of any adverse side effects that might accompany the administration of a particular composition. Typically, an attending physician will decide the dosage of the pharmaceutical composition with which to treat each individual subject, taking into consideration a variety of factors, such as age, body weight, general health, diet, sex, compound to be administered, route of administration, and the severity of the condition being treated.

**[0055]** As used herein, the terms “effective amount” or “sufficient amount” are equivalent phrases which refer to the amount of a therapy (e.g., a prophylactic or therapeutic agent), which is sufficient to reduce the severity and/or duration of a disease, ameliorate one or more symptoms thereof, prevent the advancement of a disease or cause regression of a disease, or which is sufficient to result in the prevention of the development, recurrence, onset, or progression of a disease or one or more symptoms thereof, or enhance or improve the prophylactic and/or therapeutic effect(s) of another therapy (e.g., another therapeutic agent) useful for treating a disease, such as a neoplastic disease or tumor.

**[0056]** As noted above, compositions comprising the p50-IMC of the invention can be administered parenterally by injection, infusion or implantation (subcutaneous, intravenous, intratumor, intraperitoneal, or the like) in dosage forms, formulations, or via suitable delivery devices or implants containing conventional, non-toxic pharmaceutically acceptable carriers and adjuvants.

**[0057]** In a preferred embodiment, the dosage form of the p50-IMC is suitable for injection or intravenous administration.

**[0058]** Exemplary methods for making the p50-IMC of the present invention.

**[0059]** 1) p50-IMC from p50-/- mice.

**[0060]** Bone marrow is flushed from the extremity bones and subjected to red blood cell lysis using ammonium chloride. Lineage-negative (Lin-) cells are isolated using a magnetic column, a chemical affinity column, or flow cytometry sorting, after staining with a cocktail of antibodies (e.g. targeting CD3, B220, CD11b, Gr-1, and Ter119) that bind mature blood cells. Alternatively, CD34+ cells are isolated by staining with CD34 antibody followed by affinity column chromatography or flow cytometry. The Lin- or CD34+ cells are then expanded for 6-16 days in IMDM media with 10% heat-inactivated fetal bovine serum (HI-FBS) and the FL (30 ng/mL), TPO (10 ng/mL), and SCF (30 ng/mL) cytokines, with 1x penicillin-streptomycin (P/S). These cytokines maintain cell immaturity. The cells are then transferred to IMDM with 10% HI-FBS, 1X P/S, and M-CSF (10 ng/mL) or GM-CSF (10 ng/mL) or GM-CSF (10 ng/mL) with IL-4 (10-40 ng/mL) for 1-2 days in ultra-low attachment plates, inducing formation of immature myeloid cells.

**[0061]** 2) p50-IMC from human bone marrow.

For clinical application, CRISPR/Cas9 can be used to knockout (KO) the p50 gene to generate human p50-IMC. In addition, p50 shRNA can be used to knockdown (KD) the p50 RNA to generate human p50-IMC. CD34+ hematopoietic stem and progenitor cells would be isolated from patient bone marrow or peripheral blood, for example using nanobead-conjugated CD34 antibody and immunomagnetic selection.[17] These cells will then be expanded for 6-16 days (and potentially longer), preferably in serum-free medium such as X-Vivo-20 with FL (30-100 ng/mL), TPO (10-100 ng/mL), and SCF (30-100 ng/mL) cytokines, potentially under hypoxic (e.g. 5% oxygen) conditions, and potentially in the presence of additional biologic agents. Lentiviral vectors (LV) expressing either Cas9/sgRNA (for KO) or shRNA (for KD) designed to target human p50 will be packaged in 293T cells using pMDLg/pRRE, pRSV-Rev, and pMD2.G, or related LV packaging plasmids, followed by

concentration of cell supernatants. CD34+ marrow cells will then transduced for 2-3 days as they expand using purified LV with Retronectin-coated plates, via spinoculation, or in liquid culture, potentially in the presence of 4-8 μg/mL protamine sulfate.[18] As a second method for p50 gene KO, Cas9 protein can be combined with HPLC-purified 100 bp sgRNA having 2'-O-methyl and phosphorothioate stabilizing modifications on three 5' and 3' nucleotides, e.g. in a 1:2.5 molar ratio, to generate ribonucleoprotein complexes (RNPs), followed by nucleofection into CD34+ cells as they expand.[19] Additional methods for p50 gene KO include co-nucleofection of chemically stabilized sgRNA and Cas9 mRNA or nucleofection of plasmids encoding Cas9 and p50 sgRNAs.[19,20] Use of two sgRNAs targeting different segments of the p50 gene might be used in each of these methods of p50 gene KO. After p50 gene KO or KD and cell expansion, the cells will be transferred to serum-free media with myeloid cytokines such as M-CSF (10-100 ng/mL), GM-CSF (10-100 ng/mL), or GM-CSF (10-100 ng/mL) with IL-4 (10-100 ng/mL) or FL (10-100 ng/mL) for 1-3 days prior to cell infusion. We are currently utilizing p50 gene KO, using sgRNAs cloned into LentiCRISPRv2 LV, and p50 mRNA KD, and using shRNAs in pLKO.1 LV, in the M1 murine and human U937 myeloid cell lines and in murine marrow cells expanding in TPO/FL/SCF.

**[0062]** The following examples have been included to provide guidance to one of ordinary skill in the art for practicing representative embodiments of the presently disclosed subject matter. In light of the present disclosure and the general level of skill in the art, those of skill can appreciate that the following examples are intended to be exemplary only and that numerous changes, modifications, and alterations can be employed without departing from the scope of the presently disclosed subject matter. The synthetic descriptions and specific examples that follow are only intended for the purposes of illustration, and are not to be construed as limiting in any manner to make compounds of the disclosure by other methods.

## EXAMPLES

**[0063]** Generation of murine WT-IMC or p50-IMC.

**[0064]** The inventive progenitor cell products are generated as follows: Bone marrow from WT or p50-/- mice is flushed from the extremity bones and subjected to red blood cell lysis using ammonium chloride. Lineage-negative cells are isolated using a magnetic column after staining with a cocktail of biotin-anti-Lineage antibodies (CD3, B220, CD11b, Gr-1,

and Ter119) that bind mature blood cells, and anti-biotin microbeads. The obtained Lin- cells are then expanded for 6 days in IMDM media with 10% heat-inactivated fetal bovine serum (HI-FBS) and the 30 ng/mL FL, 10 ng/mL TPO, and 30 ng/mL SCF cytokines, with 1x penicillin-streptomycin (P/S). The cells are then transferred to IMDM with 10% HI-FBS, P/S, and 10 ng/mL M-CSF for 1 day in ultra-low attachment plates. Cell morphology is assessed by Wright's-Giemsa staining of cell cytospins. Cell surface marker expression is assessed by flow cytometry (FC) using anti-CD45-BV650, anti-FLT3-BV421, anti-MCSFR-PE, and anti-CD11c-PE-Dazzle (Biolegend) and anti-CD11b-PerCPCy5.5 (BD) antibodies.

**[0065]** GBM cell inoculation and tumor monitoring.

**[0066]** GL261-Luc cells are grown in DMEM with 10% FBS. Mice are anesthetized with intraperitoneal (IP) ketamine/xylazine; the dorsal neck is shaved and sterilized and a 1 cm sagittal cranial incision is made to expose the skull; a burr hole is drilled 0.1 mm anterior and 2.25 mm lateral to the bregma; a 10 μL syringe with a 27g needle is inserted to 4 mm and 1.3 x $10^5$ GL261-Luc cells injected over 15 min; the incision is closed with a staple and adhesive. Glioblastoma tumor growth is monitored by IVIS imaging.

**[0067]** Prostate cancer cell inoculation and tumor monitoring.

**[0068]** When SQ Hi-Myc prostate cancer (PCa) tumors reached 1.2-1.5 cm, mice are euthanized and tumor tissue collected, minced with a razor blade, washed with phosphate-buffered saline (PBS), resuspended in 5mL DMEM/F12 media containing 10% FBS, 500 μL Collagenase/Hyaluronidase (Stem Cell Technologies), 2.5U/mL Dispase and 0.05mg/mL DNase I, and then incubated at 37 $^oC$ for 1 hr with occasional mixing. Tumor tissue is passed through a 40 μM cell strainer with the aid of a syringe plunger. Cells are then pelleted at 350 g x 5 min and resuspended in phosphate-buffered saline (PBS). Live cells are enumerated using Trypan Blue dye and a hemocytometer, and 2 x $10^6$ viable cells in 100 μL PBS are injected SQ into the shaved flank of mice anesthetized with isofluorane. Tumor growth is monitored using caliper measurements of length (L), width (W) and height (H), with volume estimated from the ellipsoid volume formula: $V = L \times W \times H \times \pi/6$.

**[0069]** Pancreatic cancer cell inoculation and tumor monitoring.

**[0070]** PDC-Luc cells are grown in DMEM with 10% FBS. Mice anesthetized with ketamine/xylazine are subjected to hair removal and disinfection of the operative site with Providone Iodine/Alcohol. A 1 cm incision is made in the left flank using a sterile scalpel and a 5 mm incision in the peritoneum. The entire pancreatic body together with spleen is pulled out and exposed to the outside of the peritoneal cavity by using a pair of blunt-nose

forceps. 0.5 x $10^6$ PDC-Luc cells in 40 μL Matrigel is injected using a 30g needle and a Hamilton syringe into the tail of the pancreas. The pancreas is then be returned to the peritoneal cavity with blunt forceps. The muscle layer and skin are closed separately with 4-0 absorbable sutures. Pancreatic cancer tumor growth is monitored by IVIS imaging.

**[0071]** Treatment of tumor-bearing mice with 5FU alone or with IMC.

**[0072]** 5FU is given IP at 150 mg/kg. Tail vein infusions of PBS, 1 x $10^7$ WT-IMC, or 1 x $10^7$ p50-IMC are given starting 5d after the dose of 5FU and then every 2-4 days for three total doses. Tumor growth and murine survival is then monitored.

**[0073]** Tumor myeloid and T cell isolation.

**[0074]** Prostate cancer or pancreatic cancer tumors are dissociated using 500 μL Collagenase/Hyaluronidase (Stem Cell Technologies), 2.5U/mL Dispase and 0.05mg/ml DNase I, and subjected to FC analysis, gating on live cells lacking staining with Live/Dead Aqua (ThermoFischer).

**[0075]** Tumor, node, marrow, and spleen myeloid and T cell subset and activation.

**[0076]** Spleen and lymph node cells are dissociated by passage through 40 μM cell strainers. All antibody staining is preceded by 15 min of 1:50 FcγR block in FC buffer, on ice. Extracellular antibodies are then added for 45 min on ice. Intracellular staining is accomplished after surface staining using the Foxp3 staining kit (eBioscience). Myeloid subsets are stained with anti-CD11b-FITC, anti-CD45-BV650, anti-Ly6C-AF700, anti-MR-PE-Cy7, anti-CD11c-PE/Dazzle594, anti-Ly6G-BV605 (BioLegend), anti-MHCII-eFluor450 (eBioscience), and anti-F4/80-APC (BioRad). To assess T cell activation, total tumor cells are incubated for 4 hr at 37 $^oC$ in a 5% $CO_2$ incubator with Protein Transport Inhibitor Cocktail containing brefeldin A and monensin (eBioscience). Cells are then stained with anti-CD3-AF488, anti-CD4-PE, and anti-CD8-PerCP-Cy5.5 followed by intracellular stain with anti-IFNγ-APC (BioLegend). Anti-CD45.1-PE-Cy7 and anti-CD45.2-BV650 antibodies are employed to distinguish CD45.2+ IMC from CD45.1+ host cells.

**[0077]** Western blot analyses.

**[0078]** Total cellular proteins prepared in Laemmli sample buffer are subjected to Western blotting using p50 (13586, Cell Signaling) and β-actin (AC-15, Sigma) antibodies.

**[0079]** Data analysis.

**[0080]** Prostate tumor growth is analyzed using Multiple Comparisons of Means: Tukey Contrasts. T cell subsets are compared using the Student t test.

**[0081]** Animal source.

**[0082]** WT C57BL/6 (B6) mice are obtained from Charles River Laboratories, Nfkb1(p50)-/- and CMV-Luc mice are from Jackson Laboratory (stock #s 6097, 25854).

**[0083]** Cell lines.

**[0084]** Hi-Myc PCa cells were developed from a metastatic prostate cancer lesion that formed in B6 mice expressing c-Myc from the probasin promoter.[9]
GL261-Luc cells were obtained from Perkin Elmer. UN-KC-6141 PDC cells[12] were provided by Dr. Surinder K. Batra at the University of Nebraska Medical Center. These were stably transfected with the Luc2 cDNA (Promega), with G418 selection followed by isolation of subclones by limiting dilution and screening to identify one with high-level luciferase activity, designated as PDC-Luc cells.

**[0085]** Retroviral transduction.

**[0086]** DNA oligonucleotides encoding sgRNAs targeting the murine or human p50 gene were inserted into the LentiCRISPRv2 LV vector, which were then transfected into 293T cells with the pCMV-ΔR8.91 and pMD.G(VSV.G) LV packaging plasmids using Lipofectamine 2000, followed by collection of cell supernatant 2d and 3d later to obtain LV particles. These were then filtered through 0.45 μM low protein-binding filters and used to transduce M1 or U937 myeloid cells in RPMI with 10% HI-FBS in the presence of 4 μg/mL Polybrene. Cells were then cultured in the presence of 2 μg/mL puromycin to select for transduced cells. pLKO.1 LV vectors expressing shRNAs targeting p50 mRNA were packaged similarly and used to transduce Lin- murine marrow isolated from WT mice in media containing IMDM, 10% HI-FBS, 10 ng/mL TPO, 30 ng/mL FL, and 30 ng/mL SCF in the presence of 4 μg/mL Polybrene.

## EXAMPLE 1

**[0087]** Generation of p50-IMC and their localization and myeloid potential.

**[0088]** $Lin^-$ BM cells from p50-/- mice were expanded for 6d in TPO/SCF/FL in IMDM/FBS and the transferred to M-CSF in the same media for 1d to generate p50-IMC. Morphology after Wright-Giemsa staining shows blast morphology in TPO/SCF/FL and immature monocytic morphology in M-CSF (Fig. 1A). p50-IMC were subjected to FC, demonstrating that the majority of cells express the pan-hematopoietic surface marker CD45 and the pan-myeloid surface marker CD11b, and that amongst these myeloid cells ~22% are

Flt3+CD115-CD11c+ DCs and ~57% are Flt3-CD115+CD11c- monocytes (Fig 1B). WT-IMC were generated from CMV-Luc mice using the same protocol and infused (5d after a dose of 5-FU 150 mg/kg IP) into mice inoculated previously with PDC, GBM, or PCa cells (lacking Luc). Mice or cut tumors and isolated organs were imaged by IVIS 2d later, demonstrating localization of infused IMC to the tumors, as well as to lung, spleen, and bone marrow (Fig 1C). CD45.1 mice inoculated with PDC received 5FU on d7 and CD45.2+ p50-IMC on d12 and d14, followed by FC for CD11b, CD45, and CD45.2 on d16, demonstrating that at that time ~8% of tumor myeloid cells derived from p50-IMC (Fig. 1D). Mice inoculated with PCa received 5FU on d13 and p50-IMC on d18. Myeloid cell subsets were than analyzed by FC in tumor on d2 and in spleen, draining nodes, and BM, on d6, demonstrating that about 2% of tumor, 13% of marrow, 24% of spleen, and 1.4% of lymph node myeloid cells derived from p50-IMC (Fig 1E). Tumor and marrow cells were subjected to FC for F4/80;CD11c, MHCII;CD11c, or Ly6G within the CD45.2+CD11b+ myeloid subset of PCa tumor cells two days or BM cells six days after one p50-IMC infusion, demonstrating that within the tumor p50-IMC generated F4/80+ macrophages that express CD11c and MHCII, signs of an activated state (Fig. 1F).

## EXAMPLE 2

**[0089]** Effects of p50-IMC on tumor T cell activation and PD-1 expression.

**[0090]** To evaluate the effect of p50-IMC on T cell activation CD45.1+ mice inoculated with Hi-Myc PCa received 5FU on d13 followed by CD45.2+ WT-IMC or p50-IMC on days 18, 21, and 25, followed by isolation of tumor and inguinal nodes six days later. Total tumor CD8 T cells were increased 5-fold by p50-IMC (Fig. 2A), with ~2-fold increase in IFNγ+, activated CD8 T cells evident after 4 hr stimulation with PMA/ionomycin (Fig. 2B). Similarly, 7.7% of lymph node CD8 T cells expressed IFNγ after WT-IMC compared with 14.7% after p50-IMC, in response to PMA/ionomycin ($p=0.004$), and 1.8% of lymph node CD4 T cells were IFNγ+ after WT-IMC compared with 5.3% after p50-IMC ($p=0.007$, not shown). In addition, the percent of tumor CD8 T cells expressing PD-1 increased almost 2-fold after p50-IMC (Fig. 2C), supporting the potential utility of combining p50-IMC with anti-PD-1 T cell checkpoint inhibitor antibody.

## EXAMPLE 3

**[0091]** Efficacy of p50-IMC against murine prostate cancer, glioblastoma, and pancreatic cancer.

**[0092]** The efficacy of 5FU, 5FU + p50-IMC, and 5FU + WT-IMC were compared. Cells were given vial tail vein injection, 1 x $10^7$ cells/dose, 2-4 days apart, starting 5 days after a single dose of 5FU. 5FU is given to reduce marrow competition with infused IMC, to reduce tumor myeloid cell numbers as we and others have seen, [13] and to potentially release tumor neoantigens to augment immune response. Ten mice inoculated SQ with Hi-Myc PCa cells showed significantly slower tumor growth after receiving 5FU on day 13 followed by p50-IMC on days 18, 21, and 25, compared to 10 mice receiving WT myeloid cells or 5 mice receiving 5FU alone (Fig. 3A). Mice implanted orthotopically with GL261-Luc cells received 5FU on day 3, followed by no myeloid cells, p50-IMC or WT-IMC on days 8, 11, and 14, and IVIS imaging on d21. While the 5FU or 5FU+WT-IMC groups had mice with large tumors or mice that died of tumors (indicated by X), 3 of 5 mice subjected to p50-IMC ACT developed very small GBM tumors, with one having a large tumor and one having died prior to d21 (Fig. 3B). Finally, 4 of 10 mice inoculated orthotopically with PDC-Luc cells showed marked regression in tumor size in response to 5FU+p50-IMC, but not 5FU+WT-IMC or 5FU alone (Fig. 3C) - data in the left panel were obtained by providing 5FU on day 7, followed by p50-IMC on days 12, 15, and 19; data in the right panel were obtained by providing 5FU on day 3, following by WT-IMC or p50-IMC cells on days 7, 10, and 12 (note that tumor size is on a log scale).

## EXAMPLE 4

**[0093]** p50 gene knockout (KO) and mRNA knockdown (KD) in murine and human myeloid cell lines and in murine bone marrow cells.

**[0094]** We designed five murine and human p50 exon sgRNAs using a Broad Institute website[21] and introduced the corresponding oligonucleotides into the lentiCRISPRv2 plasmid, which encodes the sgRNA, hSpCas9, and puromycin-resistance. p50 protein is markedly reduced in several pooled M1 or U937 transductants after puromycin selection, suggesting biallelic KO in the majority of clones (Fig. 4A). PCR amplification of a fragment surrounding the Cas9 cut site of targeted and control cells followed by DNA sequencing and

analysis with TIDE software evaluates p50 alleles;[14] TIDE analysis of M1 lines sg2, sg3, and sg5 shows 78-93% allele KO (not shown), with U937 sg1 cells having 89.2% p50 gene KO due to DNA insertions and deletions (Fig. 4B). In addition, we have identified p50 shRNAs effective in reducing p50 protein in stably transduced, puromycin-selected murine marrow myeloid progenitors (Fig. 4C).

**[0095]** Without being held to any particular theory, it is thought that the immaturity of p50-IMC may facilitate tumor localization and also allow DC formation, which might each contribute to efficacy. While there is previously published data showing slower melanoma, fibrosarcoma, and colon cancer growth in p50-/- mice, however, these mice lack p50 in all cell types, and the present inventors demonstrate for the first time efficacy of p50-IMC ACT. Whether generation of p50-IMC cells is best done in humans using TPO/FL/SCF followed by M-CSF for 1 day or via a related protocol (e.g. using GM-CSF instead of M-CSF) and whether reducing or eliminating p50 protein expression during expansion in TPO/FL/SCF is best done using CRISPR/Cas9 or shRNA LV transduction, CRISPR/Cas9 protein, RNA, or plasmid nucleofection, or alternative approaches will need to be determined, as will assessment of what agents best synergize with human p50-IMC, e.g. 5FU, Cytoxan, MCSFR antibody, DNA methyltransferase inhibitors, checkpoint inhibitors, and/or tumor vaccines in each cancer type.

**[0096]** All references, including publications, patent applications, and patents, cited herein are hereby incorporated by reference to the same extent as if each reference were individually and specifically indicated to be incorporated by reference and were set forth in its entirety herein.

**[0097]** The use of the terms “a” and “an” and “the” and similar referents in the context of describing the invention (especially in the context of the following claims) are to be construed to cover both the singular and the plural, unless otherwise indicated herein or clearly contradicted by context. The terms “comprising,” “having,” “including,” and “containing” are to be construed as open-ended terms (i.e., meaning “including, but not limited to,”) unless otherwise noted. Recitation of ranges of values herein are merely intended to serve as a shorthand method of referring individually to each separate value falling within the range, unless otherwise indicated herein, and each separate value is incorporated into the specification as if it were individually recited herein. All methods described herein can be performed in any suitable order unless otherwise indicated herein or otherwise clearly contradicted by context. The use of any and all examples, or exemplary

language (e.g., "such as") provided herein, is intended merely to better illuminate the invention and does not pose a limitation on the scope of the invention unless otherwise claimed. No language in the specification should be construed as indicating any non-claimed element as essential to the practice of the invention.

**[0098]** Preferred embodiments of this invention are described herein, including the best mode known to the inventors for carrying out the invention. Variations of those preferred embodiments may become apparent to those of ordinary skill in the art upon reading the foregoing description. The inventors expect skilled artisans to employ such variations as appropriate, and the inventors intend for the invention to be practiced otherwise than as specifically described herein. Accordingly, this invention includes all modifications and equivalents of the subject matter recited in the claims appended hereto as permitted by applicable law. Moreover, any combination of the above-described elements in all possible variations thereof is encompassed by the invention unless otherwise indicated herein or otherwise clearly contradicted by context.

**[0100]** References

1. Ghosh S, May MJ, Kopp EB. NF-κB and Rel proteins: evolutionarily conserved mediators of immune responses. Annu. Rev. Immunol. 1998; 16:225-60.

2. Cartwright T, Perkins ND, L Wilson C. NFKB1: a suppressor of inflammation, ageing and cancer. FEBS J. 2016; 283(10):1812-22.

3. Porta C, Rimoldi M, Raes G, Brys L, Ghezzi P, Di Liberto D, Dieli F, Ghisletti S, Natoli G, De Baetselier P,Mantovani A, Sica A. Tolerance and M2 (alternative) macrophage polarization are related processes orchestrated by p50 nuclear factor κB. Proc. Natl. Acad. Sci. USA. 2009; 106(35):14978-83.

4. Lee S, Kivimae S, Dolor A, Szoka FC. Macrophage-based cell therapies: the long and winding road. J. Controlled Release 2016; 240:527-40.

5. Burger M, Thiounn N, Denzinger S, et al. The application of adjuvant autologous antravesical macrophage cell therapy vs. BCG in non-muscle invasive bladder cancer: a multicenter, randomized trial. J. Transl. Med. 2010; 8:54.

6. Weber MS, Prod'homme T, Youssef S, Dunn SE, Rundle CD, Lee L, Patarroyo JC, Stüve O, Sobel RA, Steinman L, Zamvil SS. Type II monocytes modulate T cell-mediated central nervous system autoimmune disease. Nat. Med. 2007; 13(8):935-43.

7. Koehn BH, Apostolova P, Haverkamp JM, Miller JS, McCullar V, Tolar J, Munn DH, Murphy WJ, Brickey WJ, Serody JS, Gabrilovich DI, Bronte V, Murray PJ, Ting JP, Zeiser

R, Blazar BR. GVHD-associated, inflammasome-mediated loss of function in adoptively transferred myeloid-derived suppressor cells. Blood 2015; 126(13):1621-8.

8. Ellwood-Yen K, Graeber TG, Wongvipat J, Irueala-Arispe ML, Zhang J, Matusik R, Thomas GV, Sawyers CL. Myc-driven murine prostate cancer shares molecular features with human prostate tumors. Cancer Cell 2003; 4(3):223-38.

9. Barakat DJ, Suresh R, Barberi T, Pienta K, Simons BW, Friedman AD. Absence of myeloid Klf4 reduces prostate cancer growth with pro-atherosclerotic activation of tumor myeloid cells and infiltration of CD8 T cells. PLoS One 2018; 13(1):e0191188.

10. Seligman AM, Shear MJ. Studies in carcinogenesis. VIII. Experimental production of brain tumors in mice with methylcholanthrene. Am. J. Cancer 1939; 37:364–95.

11. Maes W, Van Gool SW. Experimental immunotherapy for malignant glioma: lessons from two decades of research in the GL261 model. Cancer Immunol. Immunother. 2011; 60(2):153-60.

12. Torres MP, Rachagani S, Souchek JJ, Mallya K, Johansson SL, Batra SK. Novel pancreatic ductal carcinoma cancer cell lines derived from genetically engineered mouse models of spontaneous pancreatic adenocarcinoma: applications in diagnosis and therapy. PLoS One 2013:8(11):e8058016.

13. Vincent J, Mignot G, Chalmin F, Ladoire S, Bruchard M, Chevriaux A, Martin F, Apetoch L, Rebe C, Ghringhelli F. 5-fluorouracil selectively kills tumor-associated myeloid-derived suppressor cells resulting in enhanced T cell-dependent antitumor immunity. Cancer Res. 2010; 70(8):3052-61.

14. Brinkman EK, Chen T, Amendola M, van Steensel B. Easy quantitative assessment of genome editing by sequence trace decomposition. Nucl. Acids. Res. 2014; 42(22):e168.

15. Delaney C, Milano F, Othus M, Becker PS, Sandhu V, Nicoud I, Dahlberg A, Bernstein ID. Infusion of a non-HLA-matched ex-vivo expanded cord blood progenitor cell product after intensive acute myeloid leukemia chemotherapy: a phase 1 trial. Lancet Haematol. 2016; 3(7):e330-9.

16. Boitano AE, Wang J, Romeo R, Bouchez LC, Parker AE, Sutton SE, Walker JR, Flaveny CA, Perdew GH, Denison MS, Schultz PG, Cooke MP. Aryl hydrocarbon receptor antagonists promote the expansion of human hematopietic stem cells. Science 2010; 329(5997):1345-8.

17. Shpall EJ, Gehling U, Cagnoni P, Purdy M, Hami L, Gee AP. Isolation of CD34-positive hematopoietic progenitor cells. Immunomethods 1994; 5:197-203.

18. Rio P, Navarro S, Guenechea G, Sanchez-Dominguez R, Lamana ML, Yanez R, Casado JA, Mehta PA, Pujol MR, Surralles J, Charrier S, Galy A, Segovia JC, Diaz de Heredia C, Sevilla J, Bueren JA. Engraftment and in vivo proliferation advantage of gene-corrected mobilized CD34+ cells from Fanconi anemia. Blood 2017; 130(13):1535-42.

19. Dever DP, Bak RO, Reinisch A, Camaraena J, Washington G, Nicolas CE, Pavel-Dinu M, Saxena N, Wilkens AB, Mantri S, Uchida N, Hendel A, Narla A, Majeti R, Weinberg KI, Porteus MH. CRISPR/Cas9 β-globin gene targeting in human haematopoietic stem cells. Nature 2016; 539(7629):384-9.

20. Mandal PK, Ferreira LM, Collins R, Meissner TB, Boutwell CL, Friesen M, Vrbanac V, Garrison BS, Stortchevio A, Bryder D, Musunuru K, Brand H, Tager AM, Allen TM, Talkowski ME, Rossi DJ, Cowan CA. Efficient ablation of genes in human hematopoietic stem and effector cells using CRISPR/Cas9. Cell Stem Cell 2014; 15(5):643-52.

21. Doench JG, Fusi N, Sullender M, Hegde M, Vaimberg EW, Donovan KF, Smith I, Tothova Z, Wilen C, Orchard R, Virgin HW, Listgarten J, Root DE. Optimized sgRNA design to maximize activity and minimize off-target effects of CRISPR-Cas9. Nat. Biotech. 2016; 34(2):184-95.

Claims:

1. A synthetic hematopoietic progenitor cell or population of cells, wherein said cell or population of cells lack or have reduced nuclear factor kappa-light-chain-enhancer of activated B cells (NF-κB) p50 protein subunit.

2. The hematopoietic progenitor cell or population of cells of claim 1, wherein said cell or cells express one or more of the following cell surface markers selected from the group consisting of CD11b, CD115/MCSFR, CD14, CD64, CD16, HLA-DR, CD209, FLT3, CD11c, CD1c, CD141, CD303, CD304, CD1a, CD15, CD13, and CD33.

3. The hematopoietic progenitor cell or population of cells of claim 1, wherein said cell or population of cells are obtained from the bone marrow or blood of a mammal which was genetically modified to lack one or both copies of the gene or to have reduced levels or activity of the mRNA for the NF-κB p50 protein subunit.

4. The hematopoietic progenitor cell or population of cells of claim 1, wherein said cell or population of cells are obtained from the bone marrow or blood of mammal where the gene for the NF-κB p50 protein subunit was genetically deleted through the use of a CRISPR/Cas9 or other gene editing construct, e.g. zinc finger nuclease (ZFN) or transcription activator-like effector nuclease (TALEN).

5. The hematopoietic progenitor cell or population of cells of claim 1, wherein said cell or population of cells are obtained from the bone marrow or blood of mammal where the level or activity of the mRNA for the NF-κB p50 protein subunit was genetically reduced through the use of an shRNA, anti-sense RNA, or anti-sense DNA construct.

6. The hematopoietic progenitor cell or population of cells of any of claims 1 to 5, wherein the mammal is a mouse.

7. The hematopoietic progenitor cell or population of cells of either of claims 1 to 5, wherein the mammal is a human.

8. A pharmaceutical composition comprising any of the cells of claims 1 to 7, and a pharmaceutically acceptable carrier.

9. The pharmaceutical composition of claim 8, further comprising at least one additional therapeutic agent.

10. The pharmaceutical composition of either of claims 8 or 9 wherein the composition is in the form of a graft.

11. Use of any of the cells of claims 1 to 7, or the pharmaceutical composition of any of claims 8-10, for treatment of cancer in a subject in need thereof, comprising administering to the subject a therapeutically effective amount of said cells or said pharmaceutical compositions.

12. The use of claim 11, wherein the cancer is pancreatic ductal carcinoma, glioblastoma, or prostate carcinoma.

13. The use of claim 11, wherein the cancer is melanoma, sarcoma, or colon carcinoma.

14. Use of any of the cells of claims 1 to 7, or the pharmaceutical composition of any of claims 8-10, to treat disease consisting of aberrant cellular proliferation other than cancer, e.g. benign tumors such as hemangiomas or myeloproliferative disorders such as polycythemia vera.

15. Use of any of the cells of claims 1 to 7, or the pharmaceutical composition of any of claims 8-10, to treat infectious diseases, including those causes by bacteria, viruses, yeast or fungi, prions, protozoa, or helminths.

16. The use of claims 12-13, wherein the subject is first treated with 15-150 mg/kg 5-fluorouracil for 1-5 days and then the subject is administered $1 \times 10^5$ to $5 \times 10^8$ cells of claims 1 to 7, or the pharmaceutical composition of any of claims 8-10 comprising $1 \times 10^5$ to $5 \times 10^8$ cells, every to 2 to 10 days later.

17. The use of claims 12-13, wherein the subject is first treated with a chemotherapy agent other than 5-fluoruracil for 1-5 days and then the subject is administered $1 \times 10^5$ to $5 \times 10^8$ cells of claims 1 to 7, or the pharmaceutical composition of any of claims 8-10 comprising $1 \times 10^5$ to $5 \times 10^8$ cells, every to 2 to 10 days later.

18. The use of claims 12-13 or 16-17, wherein the subject also receives a T cell checkpoint inhibitor every 2-4 weeks targeting PD-1, PD-L1, PD-L2, CTLA-4, LAG-3, or TIM-3 beginning prior to, simultaneous to, and/or subsequent to $1 \times 10^5$ to $5 \times 10^8$ cells of claims 1 to 7, or the pharmaceutical composition of any of claims 8-10 comprising $1 \times 10^5$ to $5 \times 10^8$ cells, every to 2 to 10 days.

## ABSTRACT

The present invention provides methods for making autologous bone marrow hematopoietic progenitors lacking NF-κB p50 protein subunit (p50). The progenitor cells are expanded, exposed to a myeloid cytokine, and provided intravenously to treat various malignancies. The infused cells have the potential to generate mature granulocytes, monocytes, macrophages, and dendritic cells that are activated due to the absence of p50. Methods for the genetically manipulation of a subject's hematopoietic progenitors during the expansion phase to reduce or eliminate p50 expression are also contemplated, and these progenitor cells may be combined with other therapeutic agents to maximize efficacy.

FIGURES 1A-1F

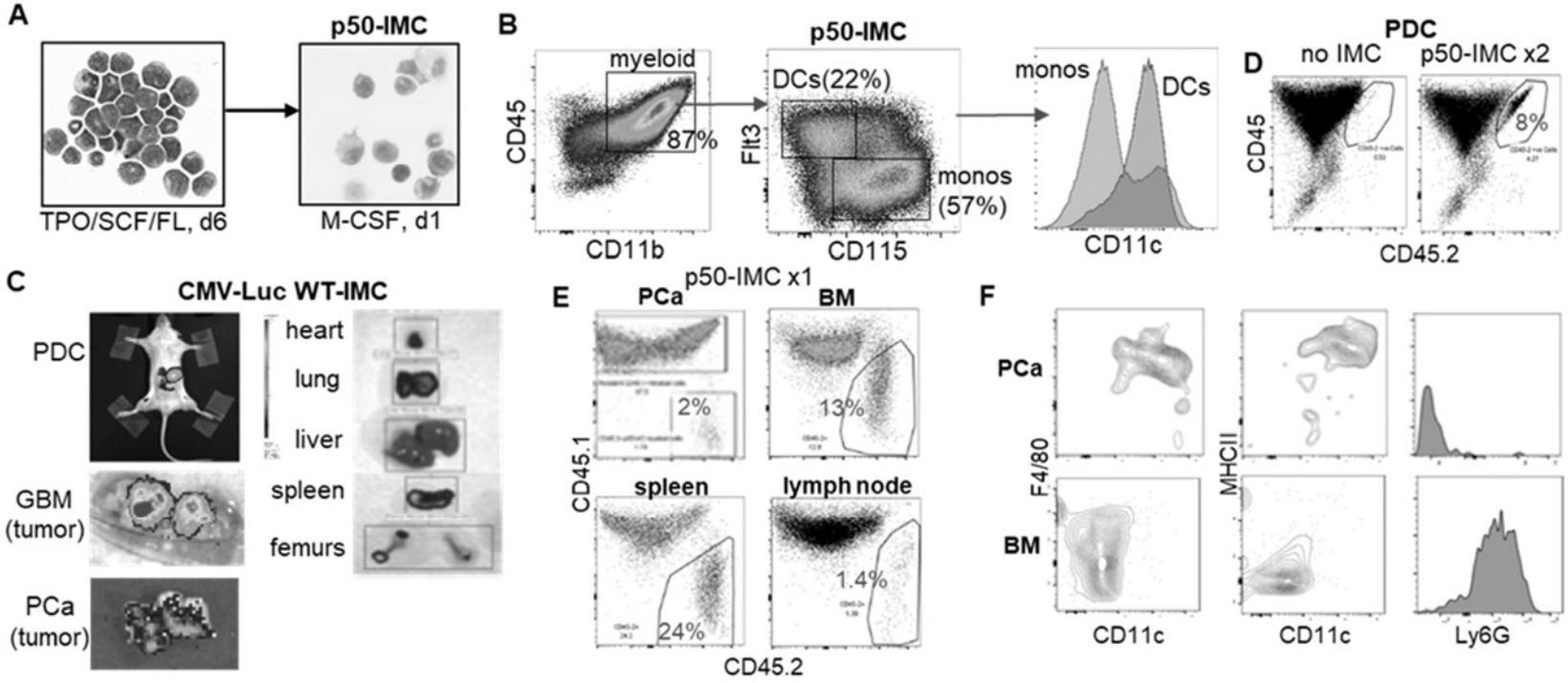

FIGURES 2A-2C

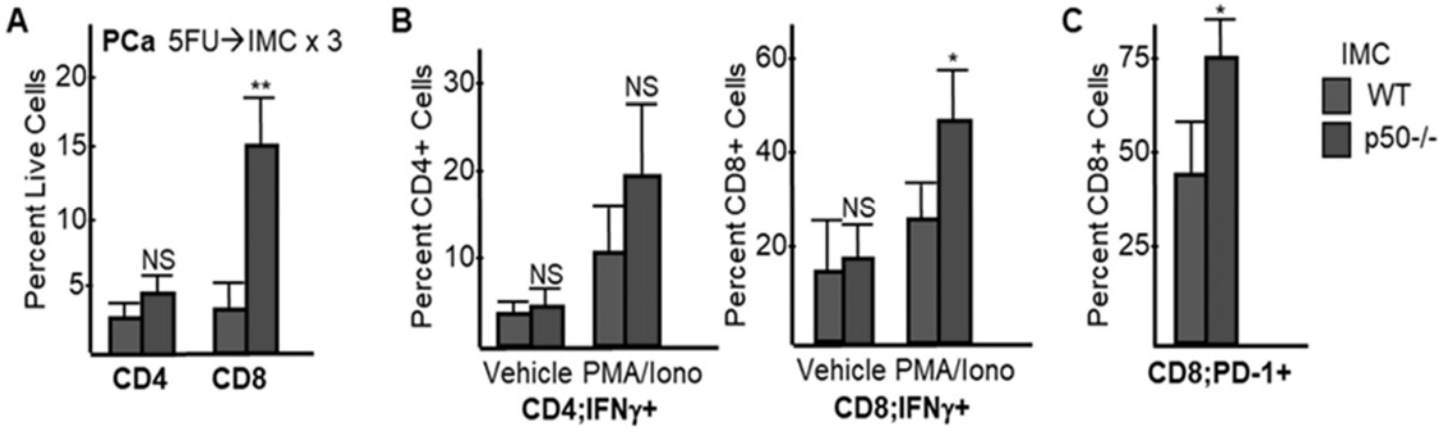

FIGURES 3A-3C

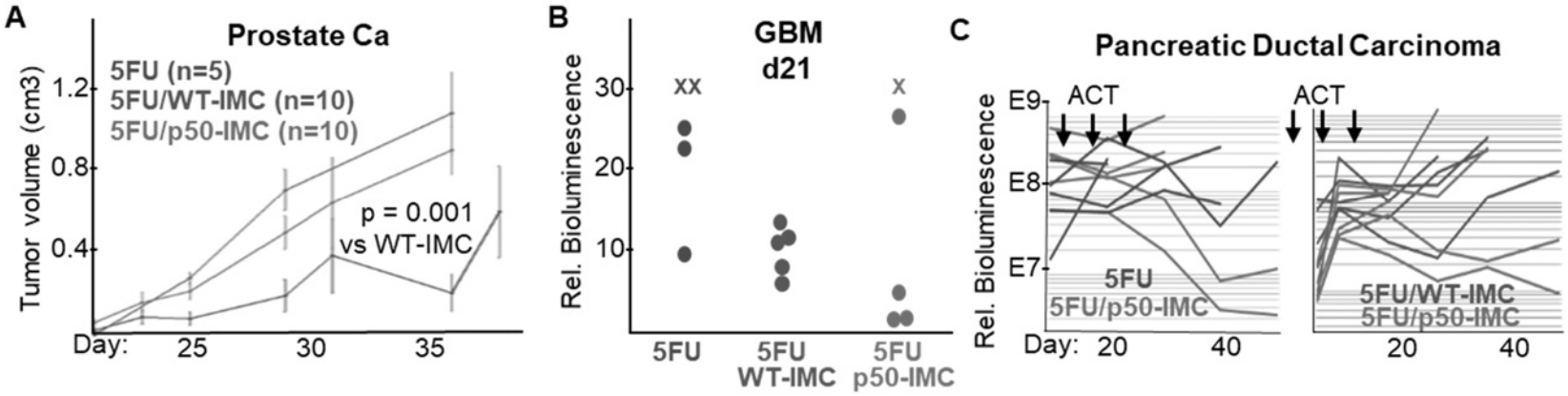

FIGURES 4A-4C